



**APPLICATION OF THE WIND GUST ESTIMATE AND
COMPARISON TO THE AFWA MM5 WIND GUST ALGORITHM**

THESIS

Kevin W. LaCroix, First Lieutenant, USAF
AFIT/GM/ENP/02M-05

DEPARTMENT OF THE AIR FORCE
AIR UNIVERSITY

AIR FORCE INSTITUTE OF TECHNOLOGY

Wright-Patterson Air Force Base, Ohio

Report Documentation Page

Report Date 11 Mar 02	Report Type Final	Dates Covered (from... to) Jun 01 - Mar 02
Title and Subtitle Application of the Wind Gust Estimate and Comparison to the AFWA MM5 Wind Gust Algorithm	Contract Number	
	Grant Number	
	Program Element Number	
Author(s) 1st Lt Kevin W. LaCroix, USAF	Project Number	
	Task Number	
	Work Unit Number	
Performing Organization Name(s) and Address(es) Air Force Institute of Technology Graduate School of Engineering and Management (AFIT/EN) 2950 P Street, Bldg 640 WPAFB OH 45433-7765	Performing Organization Report Number AFIT/GM/ENP/02M-05	
Sponsoring/Monitoring Agency Name(s) and Address(es) AFWA/DNXT ATTN: Mr. Bruce Telfeyan 106 Peacekeeper Dr. Offutt AFB, NE 68113-4039	Sponsor/Monitor's Acronym(s)	
	Sponsor/Monitor's Report Number(s)	
Distribution/Availability Statement Approved for public release, distribution unlimited		
Supplementary Notes		
Abstract The Air Force Weather Agency (AFWA) runs the Penn State/NCAR Mesoscale Model 5 (MM5) as their main mesoscale weather forecast model. One of the post-processing procedures is a diagnostic algorithm, which is used to help identify convective and non-convective wind gusts. O. Brassuer has identified a new Wind Gust Estimate (WGE), as a physically based method of computing non-convective wind gusts. The WGE surmises that Turbulent Kinetic Energy (TKE) transfers the momentum of faster upper-air winds to the surface, overcoming the buoyant energy of the surface layer. This work converts Brassuers WGE to FORTRAN code and utilizing post-processed CONUS AFWA MM5 model output to estimate wind gusts by the WGE method. The WGE and AFWA methods are then categorically compared for accuracy and skill in forecasting wind gusts, to determine if the WGE method is superior to the current method. Three geographical regions are identified to determine gust sensitivities of the WGE and AFWA algorithms. The WGE generally performs better than the AFWA algorithm during daylight hours in correctly identifying and predicting gusts. Operational use of the WGE is warranted in the day and coastal regions, while improvements to the algorithms handling of nighttime wind gusts is needed.		

Subject Terms Wind gusts, meteorological model, boundary layer, turbulence, Turbulent Kinetic Energy, wind, weather.	
Report Classification unclassified	Classification of this page unclassified
Classification of Abstract unclassified	Limitation of Abstract UU
Number of Pages 98	

The views expressed in this thesis are those of the author and do not reflect the official policy or position of the United States Air Force, Department of Defense, or the U. S. Government.

AFIT/GM/ENP/02M-05

APPLICATION OF THE WIND GUST ESTIMATE AND COMPARISON TO THE
AFWA MM5 WIND GUST ALGORITHM

THESIS

Presented to the Faculty
Department of Engineering Physics
Air Force Institute of Technology
Air University
Air Education and Training Command
In Partial Fulfillment of the Requirements for the
Degree of Master of Science

Kevin W. LaCroix, B.S.

First Lieutenant, USAF

March 2002


APPROVED FOR PUBLIC RELEASE; DISTRIBUTION UNLIMITED

APPLICATION OF THE WIND GUST ESTIMATE AND COMPARISON TO THE
AFWA MM5 WIND GUST ALGORITHM

Kevin W. LaCroix, B.S.

First Lieutenant, USAF

Approved:



Michael K. Walters
Advisory Committee Chairman

11 MAR 02

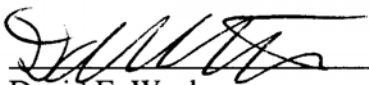
Date



Gary R. Huffines
Advisory Committee Member

11 Mar 2002

Date



David E. Weeks
Advisory Committee Member

11 Mar 2002

Date

Acknowledgements

I would like to thank Lt. Col. Walters for letting me choose my own path to enlightenment. The guidance he provided set me on the course of numerical models, and showed me that they are not to be feared, but used in ways they never were designed for. Thanks to Maj. Huffines, the reams of data downloaded and taking up space on the machines and on the shelves are because of you. I'd also like to thank MSgt. Stephen Foster of the AFCCC for his prompt delivery of critical data. Thanks to all the people who made this work better along the way. Most importantly I'd like to thank my family for all the moodiness and long boring days with nothing to do. I promise to make it up to you!

Kevin W. LaCroix

Table of Contents

	<u>Page</u>
Acknowledgements	iv
List of Figures	vii
List of Tables.....	ix
Abstract	x
I. Introduction.....	1
Introduction	1
Problem Statement and Objective	3
Importance of Investigation	4
II. Background.....	6
Description and Modeling of the Atmospheric Boundary Layer.....	6
MM5 and Boundary Layer Parameterization Description	9
Climatological Factors Affecting Peak Horizontal Momentum Methods	12
Methods of Wind Gust Estimation.....	15
Empirically Derived Estimates of Wind Gusts	16
Computational Methods of Determining Wind Gusts.....	17
ETA Second-Level.....	17
WGE Method	18
III. Methodology	23
Data Format.....	23
Computation of WGE.....	24
Computation of TKE.....	24
Computation of Buoyancy Term.....	25
AFWA Wind Gust Algorithm Description	26
IV. Data and Analysis	28
Verification of Data.....	28
Data Assimilation and Verification Procedures	28
06 UTC AFWA MM5 Model Run.....	32
18 UTC AFWA MM5 Model Run.....	47
Quantitative Comparison of the WGE and AFWA Wind Gust Algorithms	57

	<u>Page</u>
V. Conclusions	60
Summary of Results	60
Further Research Directions.....	62
Appendix A. Statistical Analysis of Two-by-two Matrices	64
Appendix B. The 06 UTC AFWA MM5 WGE and AFWA Wind Gust Forecast Verification.....	67
Appendix C. The 18 UTC AFWA MM5 WGE and AFWA Wind Gust Forecast Verification.....	76
References	85
Vita	87

List of Figures

<u>Figure Number</u>	<u>Page</u>
1. MM5 Model Windows Worldwide	2
2. Diurnal Boundary Layer Over Land	7
3. Turbulent Kinetic Energy in the Surface Layer	8
4. Schematic of 16 Sigma Levels	12
5. Shaded relief map of CONUS with Verification stations indicated with dots	29
6. Terrain heights of the CONUS T02B MM5 window	30
7. Close up of Southern Arizona Terrain	30
8. WGE 06 UTC run showing the CSI, POD, and FAR	34
9. AFWA 06Z run showing the CSI, POD, and FAR	34
10. Comparison of the Bias between the WGE and AFWA Algorithms 06 UTC run.....	35
11. Differencing of WGE-AFWA Skill Scores 06 UTC run	37
12. WGE Wind Gust Algorithm forecast 30 Oct 2001 valid 00 UTC	38
13. AFWA Wind Gust Algorithm forecast 30 Oct 2001 valid 00 UTC.....	38
14. Synoptic map of CONUS valid at 00 UTC 30 Oct 2001	39
15. 12 UTC 29 Oct 2001 Synoptic Weather Map.....	39
16. WGE Wind Gust Algorithm Forecast Valid 12 UTC 29 Oct 2001	40
17. AFWA Wind Gust Algorithm Forecast Valid 12 UTC 29 Oct 2001	40
18. Differencing of WGE and AFWA Coastal Zone Stations Categorical Scores at 06 UTC	43
19. Differencing of WGE and AFWA Plain Zone Stations Categorical Scores at 06 UTC	44
20. Comparison of WGE and AFWA Bias Scores Coastal Zone Stations 06 UTC	45

21. Comparison of WGE and AFWA Bias Scores Plain Zone Stations 06 UTC	45
22. Differences of Skill Scores WGE-AFWA Coastal Zone Stations 06 UTC	46
23. Differences of Skill Scores WGE-AFWA Plain Zone Stations 06 UTC	46
24. Differences of Categorical Scores WGE-AFWA for the 18 UTC Run	48
25. Differences of WGE-AFWA Skill Scores 18 UTC Run.....	48
26. Comparison of the Bias between the WGE and AFWA algorithms 18 UTC run.....	49
27. WGE Wind Gust Forecast Valid 21 UTC 8 November 2001	51
28. AFWA Wind Gust Forecast Valid 21 UTC 8 November 2001	51
29. WGE Wind Gust Forecast Valid 09 UTC 22 October 2001	52
30. AFWA Wind Gust Forecast Valid 09 UTC 22 October 2001	52
31. Differences in Categorical Scores WGE-AFWA Gust Algorithms Coastal Zone Stations 18 UTC Run.....	53
32. Differences in Categorical Scores WGE-AFWA Gust Algorithms Plain Zone Stations 18 UTC Run.....	54
33. Differences in Categorical Scores WGE-AFWA Gust Algorithms Coastal Zone Stations 18 UTC Run.....	54
34. Differences in Skill Scores WGE-AFWA Values Plain Zone Stations 18 UTC Run.....	55
35. Comparison of WGE and AFWA Bias Scores Coastal Zone Stations 18 UTC	55
36. Comparison of WGE and AFWA Bias Scores Plain Zone Stations 18 UTC	56
37. 06 UTC Quantitative Comparison of the WGE and AFWA methods	58
38. 18 UTC Quantitative Comparison of the WGE and AFWA methods	58
39. Comparison of the WGE-observation values of gusts and the AFWA-observation of gusts for 06 UTC KRIC Gusts	59

List of Tables

<u>Table Number</u>	<u>Page</u>
1. Comparison of boundary layer and free atmosphere characteristics.....	6
2. Wind Gust Estimate using the SL method	21
3. Comparison of WGE to SL Methodology in Uccle, Belgium	21
4. AFWA MM5 Post-Processed variables used in the WGE Algorithm with vertical resolutions.....	23
5. Verification station list for WGE and AFWA Wind gust Comparison.....	29
6. Listing of 06Z run WGE and AFWA mean scores	35
7. Mean Skill Scores for 06 UTC Run AFWA and WGE algorithms	36
8. The 18 UTC Run Mean 2X2 Scores	49
9. The 18 UTC Run Mean Skill Scores.....	49

Abstract

The Air Force Weather Agency (AFWA) runs the Penn State/NCAR Mesoscale Model 5 (MM5) as their main mesoscale weather forecast model. One of the post-processing procedures is a diagnostic algorithm, which is used to help identify convective and non-convective wind gusts. Anecdotal evidence by operational forecasters who use this product identify the AFWA algorithm as habitually over-forecasting wind gusts.

O. Brassuer has identified a new Wind Gust Estimate (WGE), a physically based method of computing non-convective wind gusts. The WGE surmises that Turbulent Kinetic Energy (TKE) transfers the momentum of faster upper-air winds to the surface, overcoming the buoyant energy of the surface layer. This work focuses on the conversion of Brassuer's WGE to FORTRAN code and the use of post-processed CONUS AFWA MM5 model output to estimate wind gusts by the WGE method. The WGE and AFWA methods are then categorically compared for accuracy and skill in forecasting wind gusts, to determine if the WGE method is superior to the current method. Three geographical regions are identified to determine gust sensitivities of the WGE and AFWA algorithms.

The WGE generally performs better than the AFWA algorithm during daylight hours in correctly identifying and predicting gusts. Unbiased skill scores show nearly even performance to AFWA's forecast. Quantitative comparisons of the observed wind gust to the forecasted gusts of the methods show the WGE method is better than the current method. Operational use of the WGE is warranted in the day and coastal regions, while improvements to the algorithm's handling of nighttime wind gusts is needed.

APPLICATION OF THE WIND GUST ESTIMATE AND COMPARISON TO THE AFWA MM5 WIND GUST ALGORITHM

I. Introduction

1.1 Introduction

Numerical models have become one of the primary tools of meteorologists in forecasting future weather events worldwide. They provide almost any product a forecaster could use to increase the accuracy and timing of their forecasts. In particular, with the rapid increase and availability of computing resources, meteorological models have been able to advance their scale and resolution to the point of providing data down to microscale regimes. Despite the increase in supercomputing power, however, meteorologists must make a trade off between a super-fine scale high-resolution model that can produce a reasonably accurate forecast, and a model that provides fine enough resolution to accurately model mesoscale weather conditions on an operationally significant basis.

Of the many weather models run by the Air Force Weather Agency (AFWA), one is a version of the Penn State/National Corporation for Atmospheric Research (NCAR) Mesoscale Model 5 (MM5). The MM5 is a finite difference, gridded user-customizable model. The AFWA MM5 usually uses a nested grid configuration, with a 45 km resolution outer grid and a 15 km resolution inner grid. Grid resolution can be thought of as the distance between two successive points of forecasted variables, or as the vertical distance between horizontal forecast planes. AFWA typically chooses to run the MM5

model every twelve hours for a forecast length of 36 to 72 hours. Locations of AFWA MM5 model ‘windows’ are shown in Figure 1.

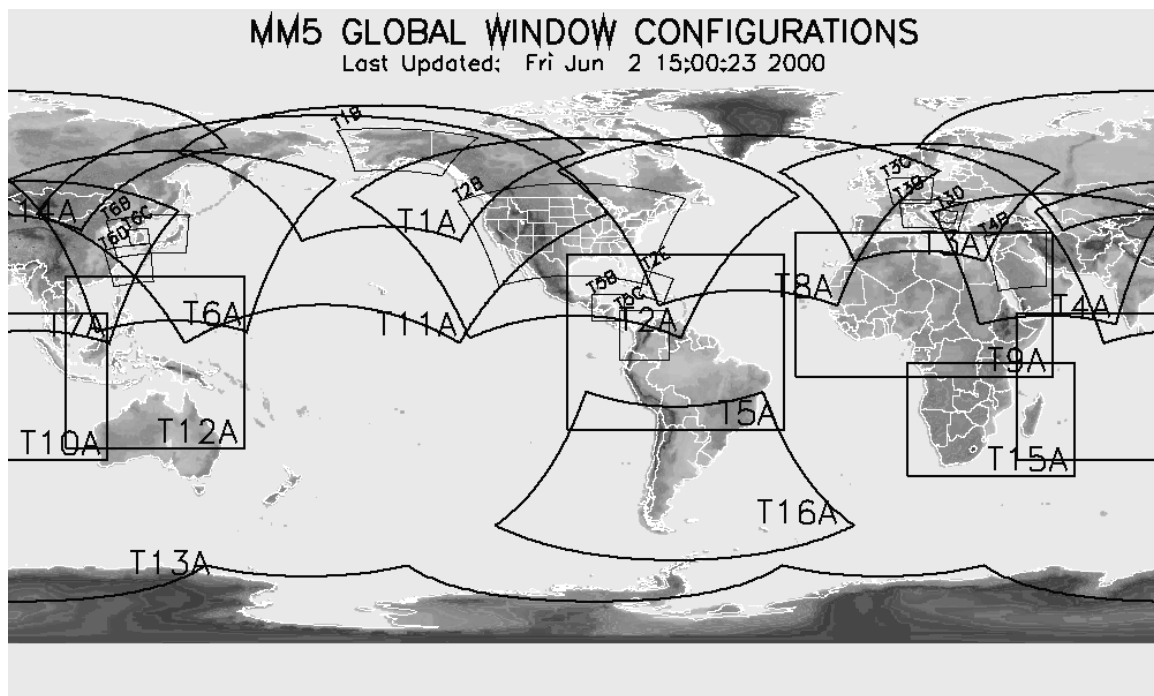


FIGURE 1. MM5 Model Windows Worldwide. Windows are identified by number and letter. The “A” windows have grid resolutions of 45 km, while “B” windows have grid resolutions of 15 km scale. (<https://www.afwin.afwa.af.mil>)

In order to accurately represent significant weather processes that occur on grid scales less than the model’s grid scale, weather modelers use parameterizations. Parameterizations are physically and empirically derived equations that attempt to model interactions occurring in real life, but which are not resolvable on the model grid. These sub-scale real- life processes can change large-scale synoptic weather patterns. The synoptic fields in turn affect primary forecast fields produced by the MM5 like temperature, moisture, and horizontal and vertical momentum. In addition to the parameterizations used in the computation of the model, post processing is accomplished on raw and derived model output data using forecast algorithms. These algorithms are like the parameterizations accomplished in the model; they take model forecast variables

and compute derived forecast fields like visibility, or wind gusts. Most of the time the algorithms involve modeling simplified physical processes, but some algorithms are exact computations and are limited only by the accuracy of the forecast fields produced by the model.

The AFWA MM5 model uses the Medium-Range Forecast (MRF) planetary boundary layer (PBL) scheme. Other PBL schemes include the Blackadar method, used by previous versions of the MM5 run at AFWA, and the Bulk-Aerodynamic parameterization (Grell et al. 1995). The MRF parameterization helps determine the horizontal and vertical temperature, moisture, and momentum fluxes in the atmospheric boundary layer (ABL). The ABL is the lowest layer in the atmosphere, where frictional forces from the surface affect the energy transfer between the surface and the upper atmosphere. The MRF improves on the Blackadar scheme by using a more descriptive land-use category surface (Hong and Pan 1996).

1.2 Problem Statement and Objective

One post-processing algorithm run by AFWA is a wind gust algorithm that parameterizes the transfer of horizontal momentum above the ABL to the surface, by looking for the first stable layer in the atmosphere computed by the model. Peak momentum transfer is directly related to the maximum wind gust recorded by observations on the surface. The AFWA algorithm depends upon the existence of a stable layer strong enough to trigger the wind algorithm. The algorithm uses the maximum horizontal momentum in the ABL to compute the wind gust. During daylight hours the top of the stable layer is not easily discerned from the model data, making the

top of the ABL unclear. Therefore, the algorithm uses the maximum potential momentum transfer through the entire column of the atmosphere, not only in the ABL, to compute the wind gust at the surface. This process results in a large overestimation of the maximum wind gust at the surface. A new algorithm that is not susceptible to the first stable layer assumption needs to be developed to reduce the overestimation of maximum wind gust and/or reduce the size of the area produced by the current wind gust algorithm.

In recent research by Brasseur (2001), he develops a new wind gust estimation method (WGE) for non-convective winds in mesoscale models. His research shows that increased horizontal resolution results in increased skill in forecasting the wind gusts, so this work will focus on the 15 km grid scale MM5. Finally, a statistical analysis of the difference between the current and proposed wind gust algorithms versus observed values of wind gusts will be made, to determine if results of the new gust algorithm actually improve the current wind gust forecast.

1.3 Importance of Investigation

Average wind speed and the maximum wind gust are critical forecasting variables for meteorologists. For Air Force weather officers in particular, concern for flight safety and protection of base property has a particular emphasis. Accurate forecasts of maximum wind gusts ensure that mission critical assets are given the necessary lead-time to implement protective measures. Air Force support for Army Aviation assets also requires accurate and timely wind gust forecasts.

Surface wind gusts affect the take-off and landing of every aircraft, especially reconnaissance aircraft like the U-2, rotary wing aircraft, and newer technological airframes like Unmanned Aerial Vehicles (UAV's). Wind gusts can cause extreme forces able to tip the airframes of large wing-surface area aircraft over while they are performing delicate maneuvers in close proximity to the ground. Army Airborne operations and Special Forces require accurate wind gust information for the safety of airborne operations. Accurate maximum wind gust forecasts are also necessary to properly employ weapon systems like the Joint Stand-Off Weapon, which may not be able to correct flight path deviations in extreme wind situations. In addition, wind gust forecasting for severe weather events affects the base assets and the safety of the people employed by the base. Events like tropical storms, hurricanes and blizzards pose significant wind gust damage hazards to Air Force bases.

It is critical that weather officers are provided enhanced techniques and tools to facilitate the Air Force's ability to project aerospace power. One of the tools desired by Air Force and DoD forecasters is an accurate method to produce maximum daily wind gust forecasts. This wind gust forecast could also be used for maximum wind gusts expected over a drop zone, strike area, or maximum wind gusts expected during a sortie. The WGE wind gust algorithm is a step in that direction.

II. Background

2.1 Description and Modeling of the Atmospheric Boundary Layer

To understand how wind gusts are formed one first has to understand the mechanisms that force the wind and how changes in the diurnal atmosphere change the wind. The troposphere can be broken down into two major layers with different dominating physical processes: the ABL, and the Free Atmosphere. Table 1 summarizes the key factors that differentiate the Boundary Layer from the Free Atmosphere.

The ABL is an important portion of the atmosphere to study because of its complexity. Transfers of momentum, water vapor, and potential temperature from the surface to the free atmosphere and back affect surface weather including wind gusts. For this work, the transfer of momentum to the surface from the free atmosphere is of major importance in determining accurate wind gusts.

TABLE 1. Comparison of boundary layer and free atmosphere characteristics (Adapted from Stull 1988)

<u>Property</u>	<u>Boundary Layer</u>	<u>Free Atmosphere</u>
Turbulence	Almost continuously turbulent over its whole depth.	Sporadic Clear Air Turbulence in thin layers of large horizontal extent.
Friction	Strong Drag against the Earth's surface. Large energy dissipation	Small viscous dissipation
Dispersion	Rapid turbulent mixing in the vertical and horizontal.	Small molecular diffusion. Often rapid horizontal transport by mean wind.
Velocity	Logarithmic Profile in Surface Layer	Geostrophic
Vertical Transport	Turbulence Dominates	Mean wind and cumulus-scales dominate

Wind gusts can be characterized as turbulent transfers of horizontal momentum from the top of the ABL to the surface. Figure 2 shows the structure of the statically stable ABL. The surface layer is the most important layer in the ABL due to frictional effects caused by viscous forces. In the daytime a convectively mixed layer lies over the surface layer, which is capped by a temperature inversion. At nighttime the convectively mixed layer transforms into a residual layer of mixed convective and stable properties. At the surface an absolutely stable nocturnal boundary layer increases in depth after sunset.

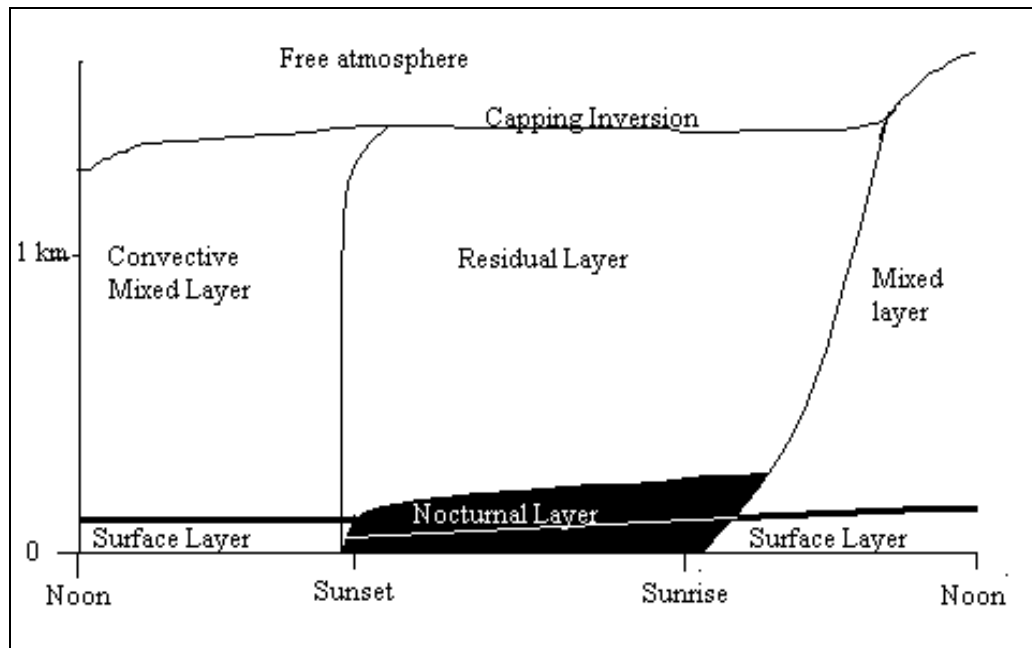


FIGURE 2. Diurnal Boundary Layer Over Land. The surface layer is affected by frictional forces while the mixed layers and residual layers have turbulent eddies. The capping inversion is the top of the ABL. (Adapted from Stull 1988)

To see how air turbulently mixes to the surface one must know the definition of turbulence. Turbulence is random and irregular fluctuations occurring in all three axes of motion. Turbulence exhibits a broad range of spatial and temporal scales from large eddies of convective nature, to those small-scale fluctuations dependent upon molecular

interactions. Turbulent Kinetic Energy (TKE) is the mean energy in an eddy of turbulent flow. Figure 3 shows a schematic of turbulence and how it mixes to the surface.

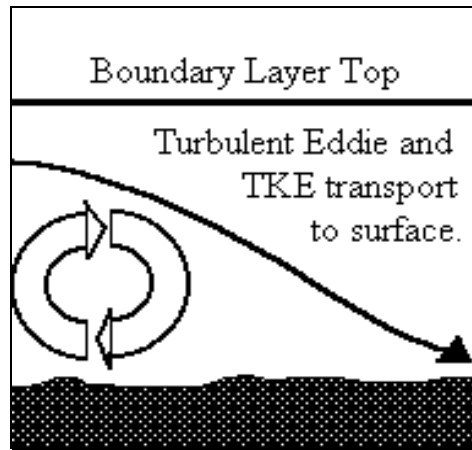


FIGURE 3. Turbulent Kinetic Energy in the Surface Layer. The turbulent eddy continuously over-turns, transporting TKE to the surface. (Adapted from Brasseur 2001)

The equations used to model the boundary layer are the Navier-Stokes equations. However, not all of the variables in the equations can be found explicitly by computational methods, because the equations are not mathematically closed. Equations with n^{th} order moments contain terms with $(n+1)^{\text{th}}$ order (Garratt 1992). Typically Reynolds averaging and closure assumptions are used to close the equation allowing the Navier-Stokes equations to be solved. The idea of Reynolds averaging is related to the fact that a variable has a mean and turbulent part.

There are two additional closure schemes, local and non-local. Local closure relates unknown quantities of turbulence to known quantities in the general flow. Non-local closure relates unknown quantities of turbulence to regions of space. Local closures have been developed, and are used routinely, to the third order (Garratt 1992). These closure terms add additional error to the final solution but are necessary for solving the Navier-Stokes equations numerically. For example, systems of three equations are used

in solving the problem, but fourth level terms are approximated in third-order closure schemes. The ABL schemes sometimes use one-and-a-half-order schemes to solve for TKE. These schemes use model variables of temperature and moisture variance along with first moment equations of momentum, resulting in three equations and six unknowns (Stull 1988). The most common closure scheme in relation to turbulent modeling is K-theory. Also known as mixing length theory, it relates thermodynamic variables to fluxes on a turbulent scale (Glickman 2001).

2.2 MM5 and Boundary Layer Parameterization Description

When computer models became useful in forecasting due to increased computational capability, it became valuable to integrate the theories of the ABL into mathematical representations solved by computer models. In addition to the computational requirements, it was difficult in the past to actually compute ABL parameterizations due to the lack of data. Radiosondes and tower measurements often do not accurately measure stability parameters and variables high enough into the ABL, or do not record measurements in all three dimensions. It was difficult to compute vertical turbulence and the transport of turbulent eddies to the surface. Computer models like the MM5, however, can estimate all the necessary variables and quantities needed for accurate evaluation of the complex models of vertical turbulent transport.

Early models had significant limitations which prevented them from developing a coherent picture of the TKE in the boundary layer. These models often did not include adequate vertical grid resolution to accurately model the ABL. The MM5 moves beyond these early operational computer models to the point that it sufficiently reproduces

environmental lapse rates and computes variables used to resolve TKE for post processing algorithms to determine forecast fields like wind gusts.

The MM5 uses numerous physical parameterizations schemes. For the ABL, the AFWA MM5 uses the MRF PBL scheme. The MRF PBL scheme was chosen for its separate soil temperature and moisture flux parameterizations. The MRF PBL scheme focuses on mechanical mixing on sigma levels to transport momentum and moisture to all points in the boundary layer.

One of the key features of the ABL is its mean climatological stability. Several stability factors have been derived to describe stability in the boundary layer. The first is the static stability factor s (Equation 1), and the second is the Richardson number, Ri , (Equation 2)

$$s = \frac{g}{T_v} \frac{\partial \Theta_v}{\partial z} \quad , \quad (1)$$

$$Ri = \frac{g}{T_v} \frac{\partial \Theta_v}{\partial z} \left| \frac{\partial V}{\partial z} \right|^{-2} \quad , \quad (2)$$

where T_v is the Virtual Temperature, Θ_v is the virtual potential temperature, V is the three dimensional wind vector, and g is the gravitational constant.

According to Arya (1988), the Richardson number is favored over the static stability factor because the Richardson number can be used in a diagnostic relationship to determine the presence of turbulence in a stratified environment. Vertical distribution of the Richardson number can help determine the vertical extent of the ABL when other methods are unavailable.

The AFWA MM5 uses 42 sigma levels in its vertical coordinate system. The model variables are mostly computed on the half-sigma levels, but the post-processing

and delivery of the AFWA MM5 forecast data reduces all variables to the whole sigma level. These 41 levels provide sufficient vertical resolution to accurately model the stable layers in the lower atmosphere. The lowest sigma levels effectively represent the ABL. Based upon fixed values at the surface and the top of the atmosphere, sigma levels are determined from a reference pressure p . Sigma values are given by the equation,

$$\sigma = \frac{(p - p_t)}{(p_s - p_t)} \quad . \quad (3)$$

p is a reference pressure at a given level, p_t is the specified constant top of the atmosphere pressure, and p_s is the surface pressure. Sigma values range from 0 at the defined top of the atmosphere (50 mb) to 1 at the surface (1000 mb). Values in parenthesis are the values used by the operational AFWA MM5 model. Figure 4 shows an example of a vertical cross section using sigma levels. (K is the sigma level number.)

Part of the improvement of the current version of MM5 from previous versions of the model is the inclusion of the ability to provide separate phase schemes for water vapor. The Reisner mixed phase parameterization allows for water vapor mixing ratios, ice mixing ratios, rain water mixing ratios, snow mixing ratios, and cloud mixing ratios (Grell et al. 1995). The saturation vapor pressure of ice and water are sufficiently different that the mixing ratios of water vapor for each phase impacts the total mixing ratio of water vapor in a given parcel of air. The complex phase parameterization impacts the computation of potential virtual temperature later in the wind gust algorithm.

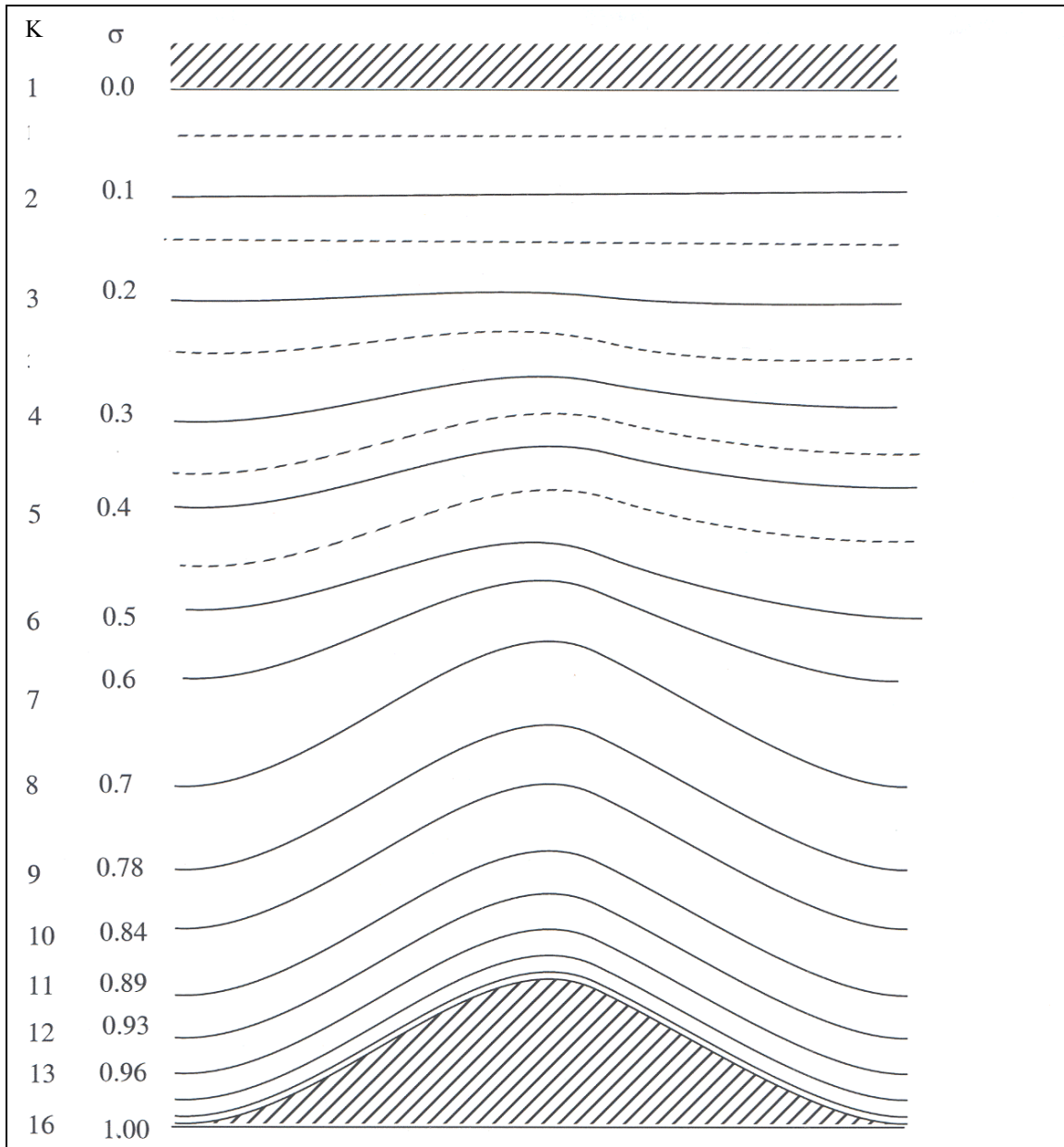


FIGURE 4. Schematic of 16 Sigma Levels. Most variables are computed on the half-sigma level. AFWA MM5 values are interpolated to sigma levels during post-processing. (Adapted from Grell et al. 1995)

2.3 Climatological Factors Affecting Peak Momentum Methods

The ABL is complex and difficult to model accurately. To determine a new wind gust algorithm, a general understanding of the ways horizontal and vertical momentum affect the overall observed wind gust must be achieved.

Following Arya (1988), the factors that influence wind distribution in the ABL are:

- Large scale horizontal pressure and temperature gradients in the lower atmosphere,
- Surface roughness characteristics, which determine surface drag and momentum exchange in the surface layer,
- The Earth's rotation,
- The diurnal cycle of heating and cooling, which determine thermal stratification,
- The ABL depth, which determines wind shear in the ABL,
- Entrainment of the free atmosphere, which determines momentum, heat and moisture exchanges at the top of the ABL,
- Horizontal advections of momentum and heat, which affect the wind and temperature profiles in the ABL,
- Large scale horizontal divergence and the resulting mean vertical motion at the top of the ABL,
- The presence of clouds and precipitation in the ABL, which influence thermal stratification, and
- Surface topography, which influence local or mesoscale circulations.

In general wind speeds in the vertical are nearly logarithmic with magnitudes varying from near zero at the surface to the full free atmospheric speed at the top of the boundary layer (Stull 1988).

Several factors affect what gust data are recorded on the daily observation sheets collected by climatological centers. Microscale statistical averages of winds and their gusts are important to understand and begin to formulate a forecast for wind gusts. The mean wind is a one-minute average of winds measured by an anemometer. Gusts are stronger winds measured during the same time period. Visually depicted on a graph of magnitude vs. time, gusts have a characteristic increase then a lull in intensity, which is Gaussian in shape. The central peak of the curve is the actual gust (Sissenwine 1973). Other factors that influence the measurement of the gusts and wind speed include the topography, the surface roughness, the height of the anemometer, which is rarely standard, and even the type of anemometer.

Significant error is introduced when trying to make comparisons between stations with different anemometer heights. Current WMO regulations prescribe a ten-meter high tower, but older weather stations had anemometers located on top of hangers, or on roofs of Weather Bureau buildings downtown. Differing anemometer locations led to climatological wind measurements ranging from one meter to over seventy-five meters high. Most researchers will extrapolate the wind speeds to ten meters, but they will usually use the logarithmic velocity profile to bring the values up, or usually down to the ten-meter level, despite all the errors assumed with the logarithmic profile theorem. In the United States, many of the current wind towers are located 10 meters high due to the implementation of the Automated Surface Observing System.

One unforeseen problem that affects the surface roughness length at a wind-recording site is the change in physical environment over time (Verkaik 2000). Growing

vegetation and encroaching buildings cause a gradual increase in the surface roughness surrounding the anemometer, causing a change in average recorded winds and gusts.

An added factor that can affect the climatology of wind gusts is the type of anemometer used and the recording system. Traditionally, a three or four-cup type anemometer is used. It works on the principle that the force on the concave sides is greater than the convex side. Another popular type of anemometer is the gill or propeller type anemometer. It works as force is applied to the helicoid rotors. The number of rotations of the rotors relate to a specific wind speed. Measurement errors of wind speeds occur when the angle of wind is not exactly matched to the direction of the anemometer. The most popular type of anemometer used for turbulence research is the sonic anemometer. It uses a timed pulse of sound modified by the wind velocity to determine the wind speed. Put into a three dimensional array, the anemometer can measure all three directions of the wind (Sorbjan 1989). When a wind recorder system is added, an error function of the response time for the anemometers is introduced. Response times for the recorders of up to five seconds are possible, meaning gusts occurring within a period of five seconds may not be recorded. Due to the inertia that the wind cups attain in a strong wind, the cups take longer to slow down to the mean wind speed when the gust is over. This forces a plot of wind gust vs. time to skew to the right of a true Gaussian shape. Finally, wind gusts are more precisely measured when the mean wind speed is already large, because the wind cups have less spin up time (Sissenwine 1973).

2.4 Methods of Wind Gust Estimation

Figure 3 shows the turbulent transport of horizontal momentum down from the free atmosphere. Stability of the lowest tenth of the atmosphere, typically the layer associated with the ABL, affects this transport of momentum. The logarithmic profile of the wind described above is an approximation, which was empirically determined. In order to make a useful forecast of wind gusts, one can apply empirically derived ways of forecasting the wind, or use atmospheric models to help develop an accurate gust estimate.

2.4.1 Empirically Derived Estimates of Wind Gusts

In the 1970's the Air Weather Service (AWS) developed several methods of forecasting wind gusts. Most of the ABL schemes assumed a statically stable stratified atmosphere, and allowed only minor convective processes. The typical wind gusts measured are non-convective in nature, however, most reliable convective data measured from radar show that the maximum-recorded surface wind gusts are convectively brought through downdrafts from 1-2 km high. AWS Technical Report 200 (Miller 1972) gives two empirical methods for determining the maximum wind gust. These methods are designed for maximum gusts that are convectively produced. These methods identify two different temperatures called T_1 and T_2 respectively. The wind gusts can be found numerically from the equation,

$$V = 13 \sqrt{\frac{T_1 + T_2}{2}} + V' \quad . \quad (4)$$

T_1 is termed the Dry Stability index, and T_2 is the downrush temperature subtracted from the dry-bulb temperature just prior to thunderstorm passage. V' is one-third the mean

wind speed in the lowest 5,000 ft. T_1 is found by following the moist adiabat from the forecast maximum surface temperature (or inversion if there is one) up to 600 mb. The temperature difference between the projected moist adiabat and the dry-bulb temperature at 600 mb is T_1 . T_2 is found by following the intersection of the moist adiabat isotherm and the wet-bulb zero degree isotherm down to the surface. The direction of the wind gust is determined by the direction of the mean wind in the 10,000 to 14,000 ft AGL layer.

Other empirical methods described in AWS TR 219 (Waters 1970) use regime based wind “boxes” based upon long term forecasting experience. However, most of the ideas included in TR 219 have become outdated.

2.4.2 Computational Methods of Determining Wind Gusts

2.4.2.1 ETA Second-Level

Hart and Forbes (1999) describe the use of the ETA forecast model to develop a methodology of non-convective wind gusts based upon hourly forecasted skew-T data. This method takes into account the increased vertical resolution of the ETA and Meso-ETA models, which allows friction to influence the boundary layer wind speeds. They show that by taking winds at the second vertical layer of the model, and statistically comparing the second level winds to observed surface winds, the second level winds more closely relate to actual gust speed than the 2-meter maximum wind speed forecasted by the ETA model. However, they note that the gust speed is highly dependent upon the model correctly predicting the static stability accurately in the boundary layer. Small differences in wind gust forecasts were noted between the Meso-ETA and the ETA

models and were attributed to the better vertical resolution of the Meso-ETA. The results of this comparison showed stronger maximum expected gusts at the surface despite the same mean wind speed in the boundary layer. Hart and Forbes (1999) conclude that this method of using the mean wind at the second model layer as an estimate of the maximum wind gust at the surface is acceptable for use in an operational sense. However, the False Alarm Rate of forecasted wind gusts of 13 m s^{-1} was close to eighty percent, for conditions with a stable inversion. This indicates that the second layer theory is sufficient for daytime use, but at night is prone to errors.

2.4.2.2 WGE Method

Olivier Brasseur of the Laboratoire d'Etude des Transferts en Hydrologie et Environnement, Domaine Universitaire, has developed a method called the Wind Gust Estimate (WGE) (Brasseur 2001). This method assumes that the maximum wind gust in the entire boundary layer can be given by

$$Wg_{estimate} = \max\left(\sqrt{U^2(z_p) + V^2(z_p)}\right) \quad . \quad (5)$$

Here z_p is the height of the parcel where TKE becomes greater than buoyancy forces and transports momentum to the surface. U and V are the horizontal components of the wind and $Wg_{estimate}$ is the wind gust by the WGE method. The critical height is found by;

$$\frac{1}{z_p} \int_0^{z_p} E(z) dz \geq \int_0^{z_p} g \frac{\Delta\theta_v(z)}{\Theta_v(z)} dz \quad , \quad (6)$$

where z_p is the critical height of a parcel, g is the gravitational constant, $\Delta\theta_v(z)$ is the vertical change in θ_v , and $\Theta_v(z)$ is the potential virtual temperature. Temperature is in Kelvin and z in meters.

Brasseur (2001) claims that a numerical model is fundamental to the process of computation of TKE in any boundary layer scheme. Brasseur used the Regional Atmospheric Model (MAR), a hydrostatic, finite difference model, in computation of the WGE (Brasseur 2001). This model produced TKE for Brasseur's computations of the WGE. Most ABL parameterizations of greater than 1.5-order closure use a diagnostic process for computing the mixing length to parameterize TKE, however TKE output is not included in the MRF PBL scheme and is not routinely included in the AFWA output. AFWA was scheduled to begin outputting TKE, but events of September 11, 2001 precluded any possibility of obtaining TKE data from the MM5 run at AFWA. Therefore an alternative method of TKE calculation was developed, and will be described in Chapter 3.

Brasseur (2001) goes a step further by developing a lower and upper bound to the wind gust. The lower WGE bound assumes that vertical variance in vertical velocity determines the wind gust, not the mean TKE in the layer as the method of vertical transport of the mean wind. Mathematically the lower bound of WGE is determined as in Equation 5 but, z_p is satisfied by

$$\frac{\overline{w'w'}(z_p)}{2} \geq \int_0^{z_p} g \frac{\Delta\theta_v(z)}{\Theta_v(z)} dz \quad . \quad (7)$$

The left hand term is half the vertical variance of the velocity as a function of parcel height z_p . Most models cannot solve for w' because it is not a prognostic variable and must be estimated. An empirically derived value of (2.5/11) times the TKE provides an empirical solution to the left side of Equation 7 (Stull 1988). Brasseur (2001) proves that the lower gust estimate is always lower than the estimated value given by Equation 5.

The maximum wind gust estimate uses the assumption that the boundary layer top is located approximately at the level where the TKE is one percent of the TKE at the surface. Using the top of the boundary layer, Equation 5 produces the upper estimate corresponding to the maximum wind speed in the boundary layer. The WGE process assumes a stably stratified atmosphere away from areas of convection. Because the WGE is non-convective in scope, this assumption poses a limitation on operational use of this tool as a single method for forecasting wind gusts. The AFWA method combines convective and non-convective wind gust methods into the total wind gust estimate.

Brasseur (2001) validates the WGE method by showing examples of the WGE applied to a study of severe cyclogenesis over Western Europe. His estimates are compared to two other non-convective methods of wind gust estimation. A summary of his results is shown in Tables 2 and 3. One method used for comparison is the gust factor, or Surface Roughness (SR). The SR method uses a constant multiplied by the mean wind speed to determine a gust over a particular surface type (Durst 1960, UK Met Office 1993, Brasseur 2001). The second method is the Surface Layer (SL) method, which uses the wind at the top of the surface layer to estimate the surface wind gust (Quinet and Nemeghaire 1991). The SL method is a variation of the method AFWA uses for non-convective wind gusts.

Brasseur (2001) shows the WGE method is generally superior to both these methods because the WGE has less reliance on stability classes, or the need for an accurate surface layer height. However, the WGE does not always outperform the SL method, as his data sometimes indicate just as relevant results for the SL method as the

WGE method. The WGE method can easily be calculated using output from NWP models, assuming the predicted TKE is available.

Some disadvantages of the WGE are related to properties of the boundary layer. Too much mechanical turbulence causes mixing of the horizontal momentum, giving an overestimated lower gust bound and estimated wind gust. An overestimated upper gust bound can occur when the boundary layer is too deep.

TABLE 2. Wind gust using the SL method. Three classes of the surface layer are determined.

Stability Classes	Wind Gust Determination
Neutral Atmosphere	Wind Velocity at top of SL
Stable Atmosphere	Wind Velocity at top of SL corrected for the effect of stable stratification
Unstable Atmosphere	Wind Velocity in the layer where the change in potential temperature with height is < 0

TABLE 3. Comparison of WGE to SL Methodology in Uccle, Belgium (Brasseur 2001) (m s^{-1})

<u>Atmospheric Situation</u>	<u>Observed Gusts</u>	<u>SL Method</u>	<u>WGE method</u>	<u>WGE Bounding Interval</u>
<u>Neutral Atmosphere</u>				
0000 UTC 2 Feb 1990	24.7	25.0	23.9	19.2-31.3
1200 UTC 7 Feb	27.2	26.1	27.0	20.6-33.6
0000 UTC 8 Feb	28.8	30.0	27.5	20.8-34.4
<u>Stable Atmosphere</u>				
1200 UTC 26 Feb	38.6	32.8	33.9	31.9-38.9
<u>Unstable Atmosphere</u>				
1200 UTC 28 Jan	29.7	22.2	10.8	9.2-14.7
1200 UTC 2 Feb	19.4	18.1	20.0	17.2-23.8
1200 UTC 12 Feb	22.5	21.1	20.6	18.1-24.1
1200 UTC 15 Feb	26.7	26.1	22.8	21.1-26.7

Brasseur (2001) notes that the 28 January 1990 under forecast of the wind is due to the WGE reliance on an accurate prediction of the surface weather pattern by the model (Table 3). In this case the MAR performed poorly in resolving the location and strength of a low-pressure system in the North Sea and consequently under-forecast the maximum winds. Accurate representation of the mean horizontal wind profiles is critical to forecasting the wind gusts. In addition to reliance on accurately predicting the moisture variables and temperature profiles, if the MM5 misplaces surface weather features like cold fronts and low-pressure centers, the WGE will under or over-forecast the wind gust using the MM5 output. Brasseur concludes that a model with increased horizontal grid resolution will provide closer wind gust estimates due to greater ability to correctly position fronts and handle mesoscale features that could be missed by grid lower resolution models.

3. Methodology

3.1 Data Format

AFWA MM5 post-processes data into GRidded In Binary data (GRIB) format in order to reduce the bandwidth needed to distribute the data over the Internet. AFWA also computes variables like thunderstorm occurrence, cloud tops, and precipitable water from the raw model output. The WGE uses many of the raw and post-processed MM5 variables on multiple vertical levels. Data were taken at the highest vertical resolution available from AFWA. Table 4 lists the variables and the vertical resolution that were used for each variable.

TABLE 4. AFWA MM5 Post-Processed variables used in the WGE Algorithm with vertical resolutions.

Variables on 41 Sigma levels	Variables on 21 Pressure levels	Variables at Surface
u,v component of wind	Pressure Vertical Velocity	Accumulated Convective Precipitation
Humidity mixing ratio	Rain Water Mixing Ratio	u,v wind at 2 meters
Cloud mixing ratio	Ice Water mixing Ratio	AFWA u,v components of windgust
Temperature		

The WGE algorithm was implemented in FORTRAN 90/95 and includes a subprogram to read in the data. Due to the length of the programs, they are not included in this work. The GRIB data were converted to binary data using Wesley Ebisuzaki's WGRIB program (Ebisuzaki 1999). WGRIB uses variable namelists to decode the GRIB data. First a namelist using AFWA GRIB variables had to be constructed, for use in

place of the NCEP default variable namelist. Data were downloaded once a day for each AFWA MM5 model run at 06 UTC and 18 UTC.

Because the variables are defined at different vertical resolutions, interpolation of the variables from pressure levels to sigma levels was accomplished in a linear manner based on height. The MM5 variables that are distributed in the AFWA GRIB file do not include the geometric vertical velocity dz/dt (w). In order to find w , ω (dp/dt) is converted to dz/dt by the approximation $\omega = -pgw$ (Holton 1992). Vertical velocity is interpolated linearly in height to the sigma levels using the reference pressure at the sigma level. The final conversion is from temperature at the sigma level to the potential temperature at that sigma level.

The WGE uses virtual potential temperature to compute the buoyancy term. Accordingly virtual potential temperature, θ_v , is computed using

$$\theta_v = \theta(1 + .61r - r_L) \quad , \quad (8)$$

where r is the humidity-mixing ratio and r_L is the sum of rain, cloud and ice mixing ratios (Glickman 2001). Virtual potential temperature is used to account for the additional cooling provided by the water content of the atmosphere as horizontal momentum is brought to the surface.

3.2 *Computation of the WGE*

3.2.1 *Computation of the TKE*

According to the WGE method, the left term of Equation 6 involves computing TKE. The TKE brings the higher velocity air of the free atmosphere down to the surface

using convective eddies. The algorithm computes the TKE at all sigma levels. It does this using several critical assumptions. First, TKE per unit mass is computed as;

$$TKE = \frac{1}{2}(\overline{u'^2} + \overline{v'^2} + \overline{w'^2}) \quad , \quad (9)$$

where u' , v' , and w' are the perturbation velocities of their respective wind components and the over-bars represent Reynold's averages (Stull 1988). According to Stull (1988), the ergodic condition is satisfied when the time, space, and ensemble averages are equal, and the turbulence is statistically not changing over time. The MM5 output is produced every three hours. To time difference the perturbations would most likely produce more errors than a space difference during the same time would, thus the ergodic condition was assumed to be satisfied allowing the use of the space average to compute the perturbation values. The algorithm computes the perturbation value of the wind as the value of the wind at the gridpoint subtracted from the average of the wind at the gridpoint and the eight surrounding gridpoints. Special consideration has been taken for the corners and the edges. The edges are computed from the wind speeds at the six closest gridpoints inclusive of the gridpoint, and the wind in the corners are calculated with the closest five gridpoints to the corner.

3.2.2 Computation of the Buoyancy Term

The buoyancy term includes the virtual potential temperature (θ_v) and the vertical change in θ_v ($\Delta\theta_v$). The buoyancy term is given by

$$\int_0^{z_p} g \frac{\Delta\theta_v(z)}{\Theta_v(z)} dz \quad , \quad (10)$$

which is the same as the right hand side of Equation 6. The computation involves creating an array of dz , which is constant because the sigma coordinates in the non-hydrostatic MM5 are set at constant altitudes over the terrain. The algorithm then creates three-dimensional arrays of the integral of the TKE and the virtual potential temperature term in Equation 10 above. The WGE then compares the integral values to find the highest level where the TKE is greater than the buoyancy.

The algorithm compares terms from the top of the atmosphere down to locate the first level where the integrated TKE does not exceed the buoyancy term. The highest level identified will typically bring the strongest possible gust to the surface since the tropospheric winds generally increase with height. The level chosen by the comparison becomes the critical height for the WGE. With this information the maximum wind in the column above the gridpoint is found and a magnitude is computed. Next, the algorithm assigns WGE gust values for twenty-three verification locations according to their grid location using grid-to-station interpolation. Finally the program formats output for display using GrADS software.

3.3 AFWA Wind Gust Algorithm Description

The current AFWA wind gust post-processing algorithm computes u and v components of the wind gust. It is a two-part algorithm, one for non-convective winds, which was tested against the WGE, with a separate section that uses the WINDEX formula to predict convective wind gusts (McCann 1994).

The convective section is triggered if the convective precipitation of the model is greater than 0.01 inches during any three-hour forecast time period. The non-convective portion uses the average wind speed in the surface boundary layer for its estimation of the wind gust magnitude. The AFWA algorithm checks to see if $d\theta/dz$ is less than zero. If so, the temperature inversion of the stable layer prevents the buoyant energy from contributing towards the formation of wind gusts. The AFWA algorithm will continue to check the successive model layers until the model-derived height of the ABL was reached. The problem with this method is that it could rely on the model ABL height to achieve a solution, if $d\theta/dz < 0$ is never satisfied. The AFWA algorithm will use the entire column of the atmosphere in the boundary layer to compute the wind gust if no stable layer is identified. The result is an overestimation of the wind gust, especially in the daytime, when the lapse rate has the climatologically greatest value.

IV. Data and Analysis

4.1 Verification of Data

The data output from the WGE algorithm was in two different forms. One was a gridded format optimized for graphical output, the other a text file of the AFWA gust, the WGE gust, and the upper bound of the WGE gust estimate. Each time the algorithm ran with model data it produced fifteen text files and fifteen gridded data files. Due to quality control, missed communication connections, and tape recovery problems only 53 different runs were analyzed. Twenty-three cities/airfields were chosen for verification. These included a large percentage of Air Force installations to highlight the variation in Air Force mission locations. The sites were also chosen for their geographic locations and the surrounding topography. In addition, sites were chosen as near to the corners of the T2B MM5 window (Figure 1) as possible to help investigate whether the WGE output was susceptible to inaccuracies based on boundary conditions. A mix of coastal, mountainous, and plain locations was selected. Five stations from each geographical section were selected to separately identify any regional differences in the WGE method over the CONUS. Figure 5 shows the locations of the sites, and Table 5 lists the pertinent details of the locations. Figure 6 shows the terrain of the T02B window. Figure 7 shows a close-up of terrain around KDMA.

4.2 Data Assimilation and Verification Procedures

Observational data were received from the Air Force Combat Climatology Center from all verification sites. The data consisted of all observations taken by the stations, including special and routine METAR observations. Peak winds not observed at the

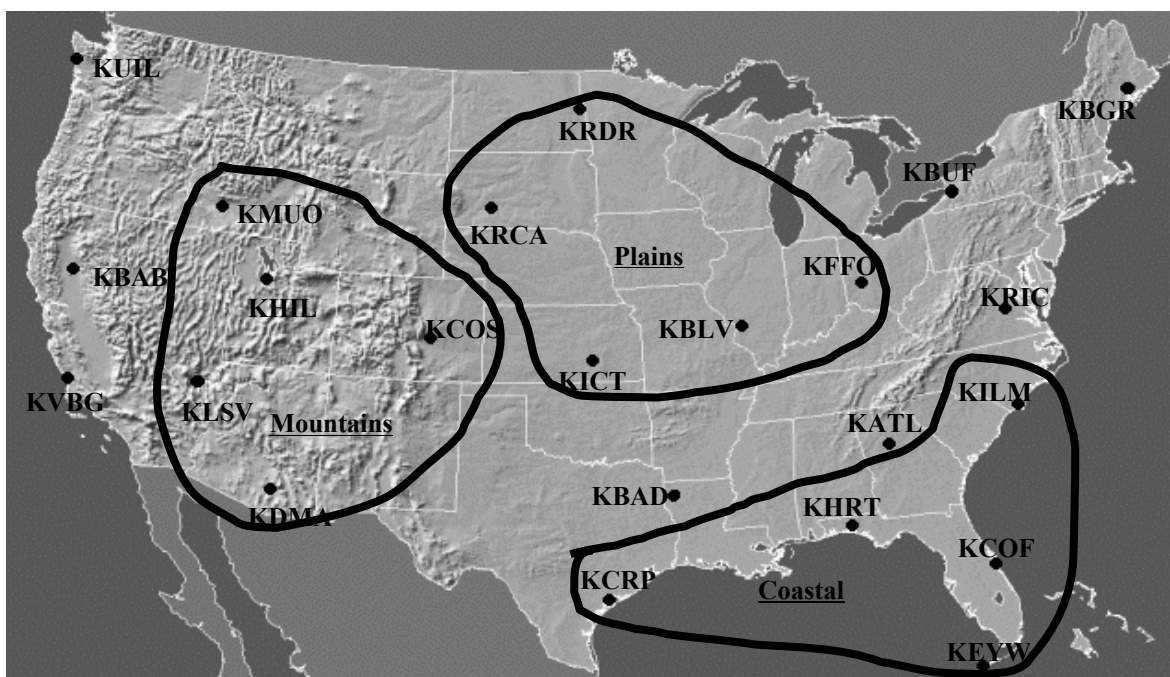
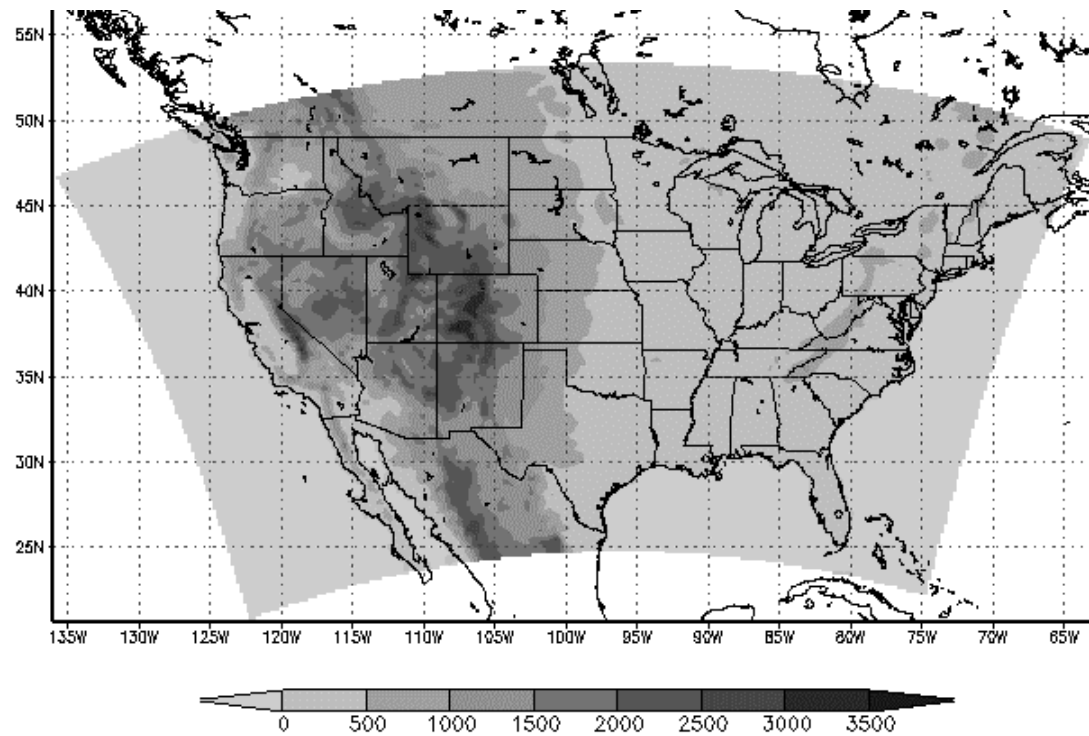


FIGURE 5. Shaded relief map of CONUS with Verification stations indicated with dots and the three geographical zones outlined.

TABLE 5. Verification station list for WGE and AFWA Wind Gust Comparison

Station Name	ICAO	Longitude	Latitude	Grid i	Grid j	Elevation (m)
Key West, FL	KEYW	-81.45	24.33	252	24	6
Wichita, KS	KICT	-97.26	37.39	180	99	408
Bangor, ME	KBGR	-68.49	44.48	312	140	59
Corpus Christi, TX	KCRP	-97.30	27.46	179	42	13
Richmond, VA	KRIC	-77.19	37.31	273	93	54
Quillayute, WA	KUIL	-124.33	47.56	54	158	62
Patrick AFB, FL	KCOF	-80.35	28.13	258	45	3
Colorado Springs, CO	KCOS	-104.43	38.49	148	106	1885
Atlanta, GA	KATL	-84.27	33.38	240	76	315
Beale AFB, CA	KBAB	-121.25	39.07	69	107	34
Vandenberg AFB, CA	KVBG	-120.34	34.38	74	80	112
Davis-Monthan AFB, AZ	KDMA	-110.52	32.10	119	67	824
Hurlbert Fld, FL	KHRT	-86.40	30.25	231	57	12
Scott AFB, IL	KBLV	-89.50	38.32	216	103	138
Mountain Home AFB, ID	KMUO	-115.52	43.02	96	130	913
Barksdale AFB, LA	KBAD	-93.40	32.40	198	68	51
Wilmington, NC	KILM	-77.54	34.16	272	79	10
Grand Forks AFB, ND	KRDR	-97.24	47.58	180	156	278
Nellis AFB, NV	KLSV	-115.01	36.13	98	90	570
Buffalo, NY	KBUF	-78.44	42.56	268	127	215
Wright-Patterson AFB, OH	KFFO	-84.02	39.49	242	110	251
Ellsworth AFB, SD	KRCA	-103.05	44.08	154	136	999
Hill AFB, UT	KHIF	-111.58	41.07	114	119	1459



GrADS: COLA/IGES

2002-03-08-10:57

FIGURE 6. Terrain heights of the CONUS T2B MM5 window. This map contrasts the shaded relief map from Figure 6. The gray shaded areas show the boundaries of the 15 km window. This is a Lambert Conic Conformal model plotted on a Mercator Map. Units in meters.

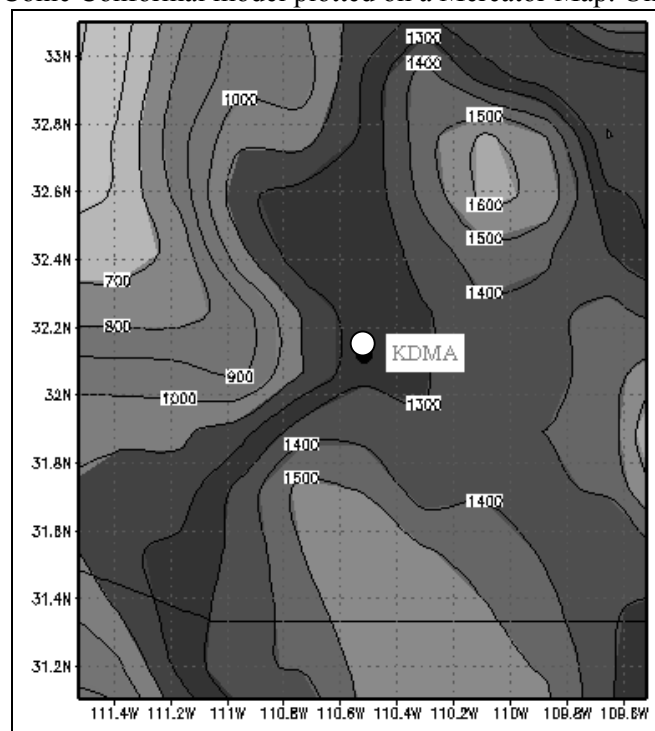


FIGURE 7. Close up of Southern Arizona Terrain
The complexity of the terrain in mountainous areas is evident in this figure. KDMA is located at the filled circle. Units in meters.

time of observation and listed only in the remarks section of the observation were not included in the verification procedure. One of the difficulties encountered with the verification of forecasts is that many of the Air Force Bases do not perform twenty-four hour observing. Therefore, during weekends and holidays, no observations were obtained for those sites. Also, many of the cities didn't have data for whole model runs. The stations with ASOS data were the most reliable, and stations that had twenty-four hour a day observing support were the best of all. Overall, KUIL, KVBG, KBAD, KHIF, and KMUO were the most likely to miss the observation.

Since observations are supposed to be taken at ten minutes to the hour, every hour, and the data from the model run only comes every three hours, only observations occurring within forty minutes of the time of the model data were accepted for verification. Forty minutes was deemed sufficient time to send corrections and allow for special observations occurring near the forecast time to be included. If two or more observations occurred within the allotted time window, the highest recorded gust during that period was taken as the gust for that station during that time. A final addition to the verification procedures used sustained winds of fifteen knots or greater as a verified wind gust. A sustained wind of 15 knots or greater was surmised to include at least a gust of the mean wind speed.

The two daily runs were treated as separate statistical entities, in order to help ensure independence was maintained. If consecutive runs were analyzed together, then six of the fifteen forecast periods would have the same verification time. With weather patterns moving slowly enough, a poor forecast of synoptic features would most likely cause the results to be dependent in consecutive forecast periods.

Where the two competing wind gust forecasts were computed with continuous results, the verification observations were discrete numbers increasing from fifteen knots and including zero. In order to analyze the results, each of the fifteen forecast time periods were broken up into separate statistical units. All the verifications occurring at that forecast period were entered into a two-by-two matrix, with forecast (yes/no) versus observed (yes/no). A yes forecast was considered to be a forecast gust of 15 knots or greater, while a yes observation was an observed gust or sustained wind of 15 knots or greater.

Each of the fifteen forecast times from the two runs were analyzed for the following criteria; False Alarm Rate (FAR), Bias, Critical Success Index (CSI), Hit Rate (HR), and Probability of Detection (POD) (Wilks 1995). A χ^2 test was accomplished on all two-by-two categorical sets to determine independence. When the χ^2 test was found to be insufficient to assume independence, a Fisher-Irwin Exact test was done to verify the significance of the result with alpha set to 0.05. In addition to the straight scoring of the two methods, three separate skill scores were computed. Appendix A details the calculations and procedures for the two-by-two tests and the skill scores.

4.3 06 UTC AFWA MM5 Model Run

The 06 UTC run had more data points because it included two more complete runs than the 18 UTC run, but due to a communications problem, the 10th forecast period at 15 UTC on the second day was corrupted. This limited the number of forecasts that could be verified at this time period. The verification data showed that the number of forecast/observation pairs produced results that were a reasonable representation of the

climatology of wind gusts. The maximum occurrence of wind gusts is in the afternoon, and the minimum of wind gusts is just prior to sunrise. Appendix B lists the scores for the 06 UTC run per forecast time.

The 24-hour period of the day was broken up into daytime and nighttime portions, with the UTC times of 15, 18, 21, and 0, considered to be during daylight hours for all locations. For the 06Z run these times are the 9-, 12-, 15-, 18-, 33-, 36-, 39-, and 42-forecast hours. The distribution of station location is slightly skewed towards the eastern US. The breakdown of verification sites versus time zones has 8 sites in the Eastern, 7 in the Central, 5 in the Mountain, and 3 in the Pacific Time Zones. This matters because the stations are all treated as being in the day or night at the same UTC time. Therefore some stations, especially in the Eastern or Pacific Zones, might still be dark/light when the other stations are light/dark.

Initial assessment of the WGE forecast results based upon a visual inspection of the data showed results similar to the AFWA model. Figures 8 and 9 show the CSI, POD, and FAR for the WGE and AFWA wind gusts from the 06 UTC MM5 run. As WGE CSI increased, the CSI for the AFWA algorithm increased as well. The values of FAR for the two methods are very high, but the AFWA method consistently scores in the 50-70% range. The WGE's FAR sometimes drops as low as 40%. The nighttime values of the WGE FAR in Figure 8 show a diurnal trend. For all comparison tables, the gray section above the data is indicative of nighttime, while the light zones are daytime.

Table 6 lists the mean scores from the two-by-two tables. The POD and the FAR have better scores from the WGE than the AFWA algorithm. The WGE performs better for positive values of difference, except FAR scores where a negative score is better.

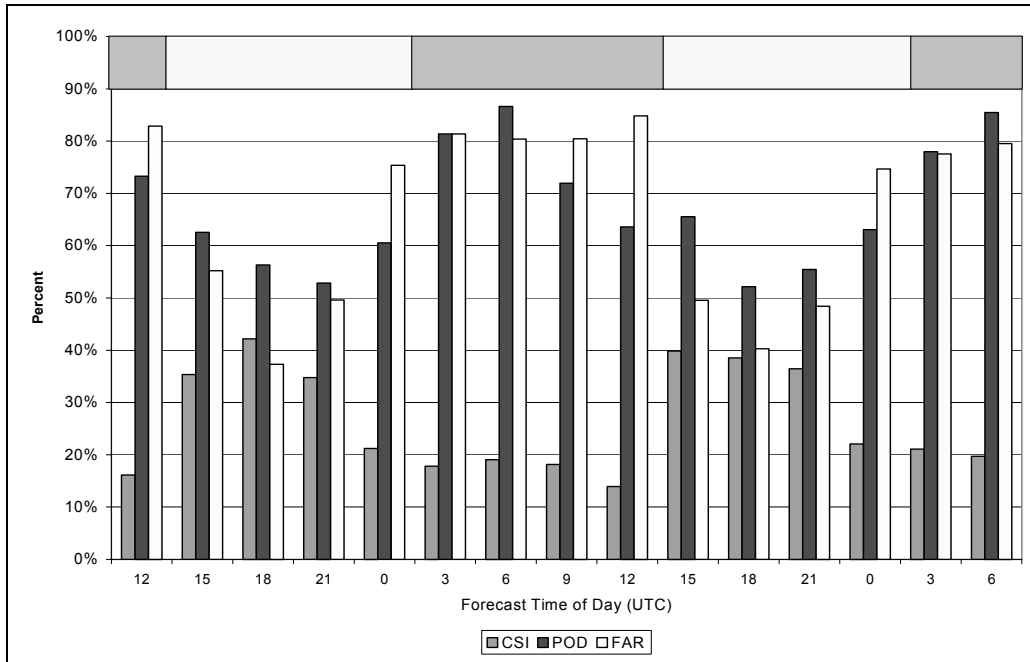


FIGURE 8. WGE 06 UTC run showing CSI, POD, and FAR. Forecast time of day is along the bottom axis, and the percentage is along the y-axis. The gray shaded regions on the top of the graph are nighttime periods during the entire forecast. All similar charts have the gray shaded nighttime areas on the top.

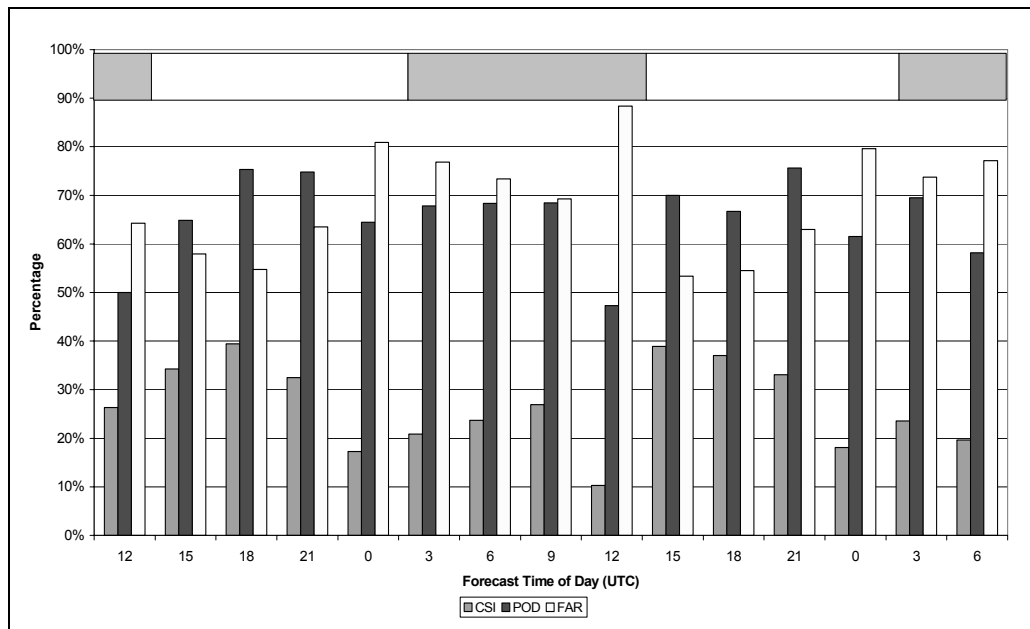


FIGURE 9. AFWA 06Z run showing the CSI, POD, and FAR (As in Figure 8).

TABLE 6. Listing of 06Z run WGE and AFWA mean scores.

	WGE	AFWA	
	raw score		difference
Hit Rate:	0.679	0.695	-0.016
CSI:	0.264	0.268	-0.004
POD:	0.673	0.655	0.017
FAR:	0.665	0.687	-0.022
BIAS:	2.677	2.337	0.341

The Bias of the two algorithms shows an interesting phenomenon. Figure 10 shows the Bias of the WGE and the AFWA algorithm in comparison. The AFWA algorithm Bias shows a more gradual change in values as the forecast period advances. Neither of the algorithms shows a worsening of forecasting ability as time increases. The WGE however, shows a drastic swing in Bias values over the entire model forecast run. An explanation for this result is the major discovery of this work.

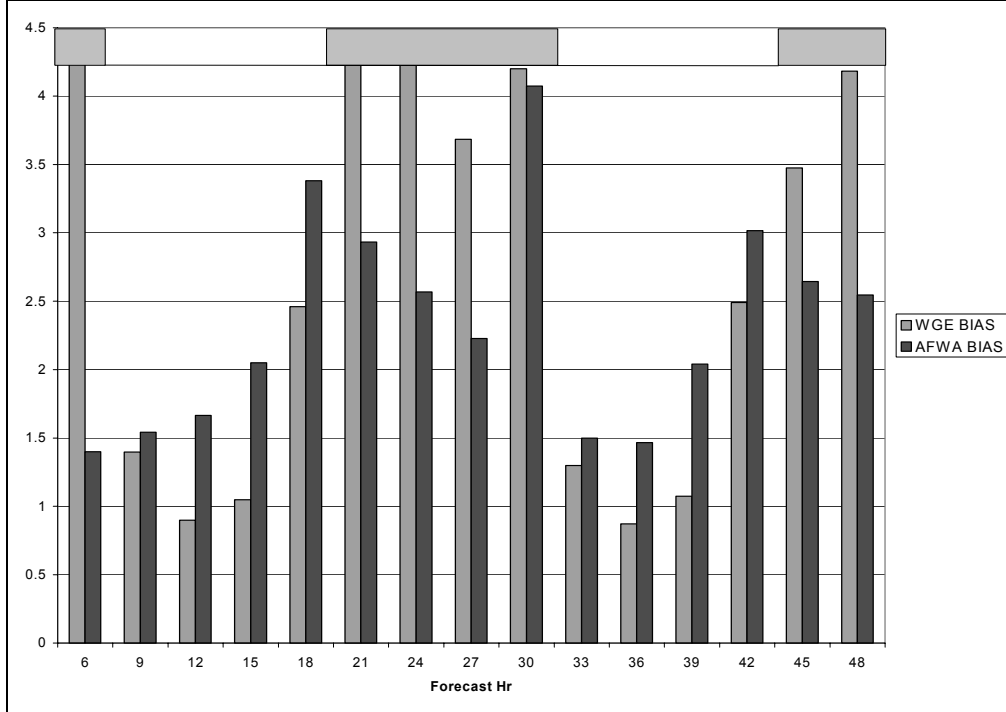


FIGURE 10. Comparison of the Bias between the WGE and AFWA Algorithms 06 UTC run. A Bias of 1 is a perfectly forecasted event. Values less than 1 indicate under-forecasting the event, and values over 1 show over-forecasting. The nighttime hours show a significant over-forecasting of wind gusts by the WGE.

Looking at the two-by-two data in Appendix B shows that the WGE has Biases that range from 0.873 to 2.492 during daylight hours, with values of Bias that range 3.475 to 4.417 during the nighttime. These drastic differences in Bias values between the day and night show that some processes of the WGE, as implemented in this research, must have trouble with nocturnal wind regimes. In contrast to the poor performance of the Bias of the WGE during the 06 UTC run, the AFWA algorithm does surprising well with Bias in the daylight hours. From evidence gathered prior to the start of the research, the AFWA Bias values in the daytime should be similar to the values of Bias of the WGE at night. However, for the 06 UTC run, Bias of the two methods show roughly the same trend to over-forecast at night and under-forecast in the day.

The differencing of skill scores for the 06 UTC WGE and AFWA algorithms are shown in Figure 11. Values of the skill scores for the AFWA algorithm are subtracted from the WGE skill scores and the result is plotted per forecast time. It is very obvious that the differences in the two algorithms break down along day and night periods. However, as Table 7 shows, the WGE has a slight advantage in skill for all types of skill score, although the differences are insignificant between the two competing algorithms.

TABLE 7. Mean Skill Scores for 06 UTC Run AFWA and WGE algorithms.

	WGE	AFWA	
	raw score		difference
HSS:	0.253	0.247	0.006
KSS:	0.369	0.353	0.016
ETS:	0.150	0.143	0.007

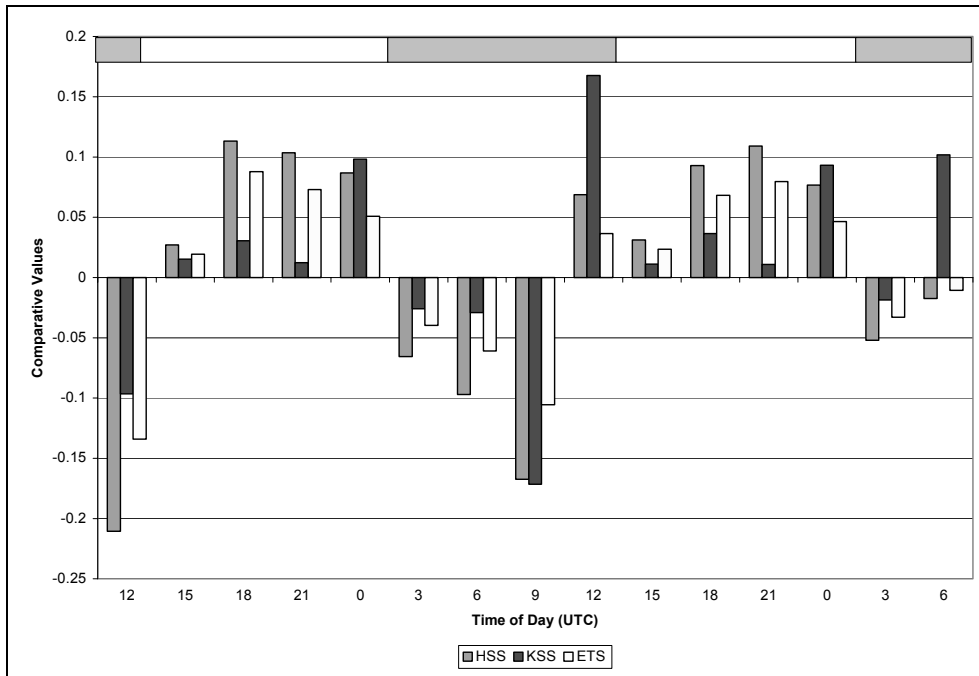


FIGURE 11. Differencing of WGE-AFWA Skill Scores for the 06 UTC run. Values greater than zero indicate scores where the WGE is better. Except for the second 12 UTC forecast period, the skills breakdown along day and night periods.

Figures 12 and 13 show the difference between the AFWA and WGE forecast algorithms with respect to a single forecast time. Figure 12 shows the 18-hour WGE forecast for the 06 UTC run for 29 October 2001 valid at 00 UTC on 30 October. Contrast this with the same valid time for the AFWA algorithm in Figure 13. The AFWA algorithm is over-forecasting wind gusts over the upper Midwest and Mississippi River valley. The WGE in contrast, does not over-forecast in these areas, but is forecasting gusty winds in the Northeast. Figure 14 shows the synoptic situation for the forecast time. The frontal placement is affecting the WGE gusts in New England, but as the high-pressure builds in behind the front in the Upper-Midwest, the AFWA gust over-forecasts. Figure 15 displays the synoptic situation for the nighttime forecasts of Figures 16 and 17. Figure 15 shows the synoptic situation 12 hours earlier than in Figure 14.

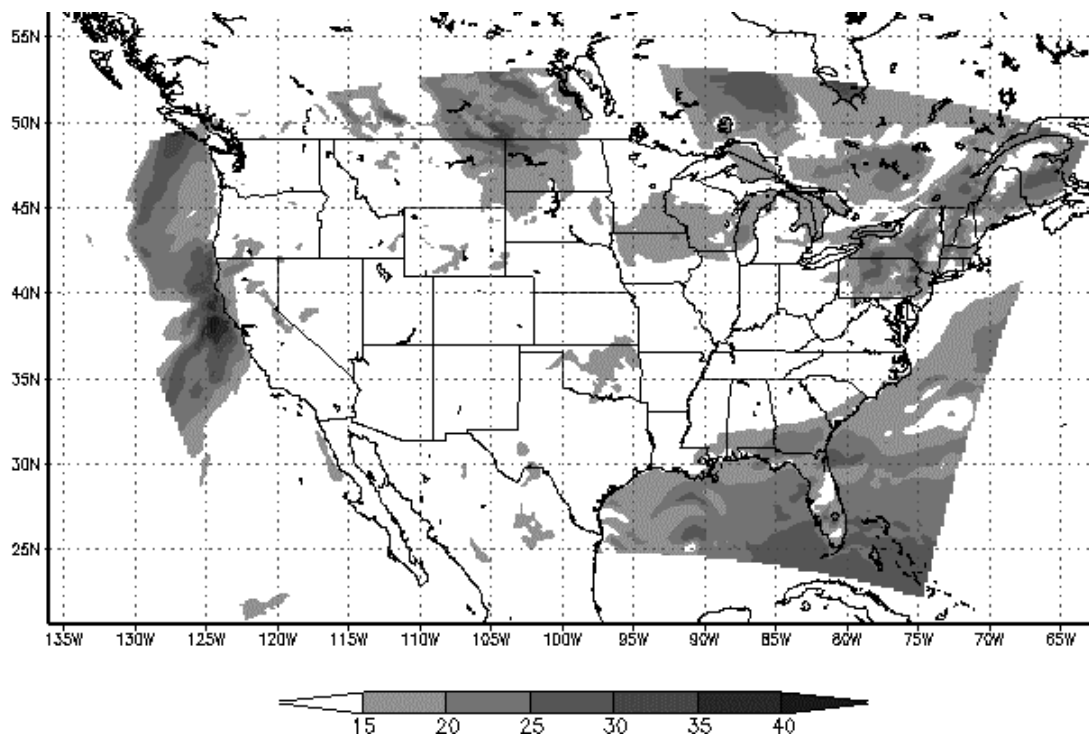
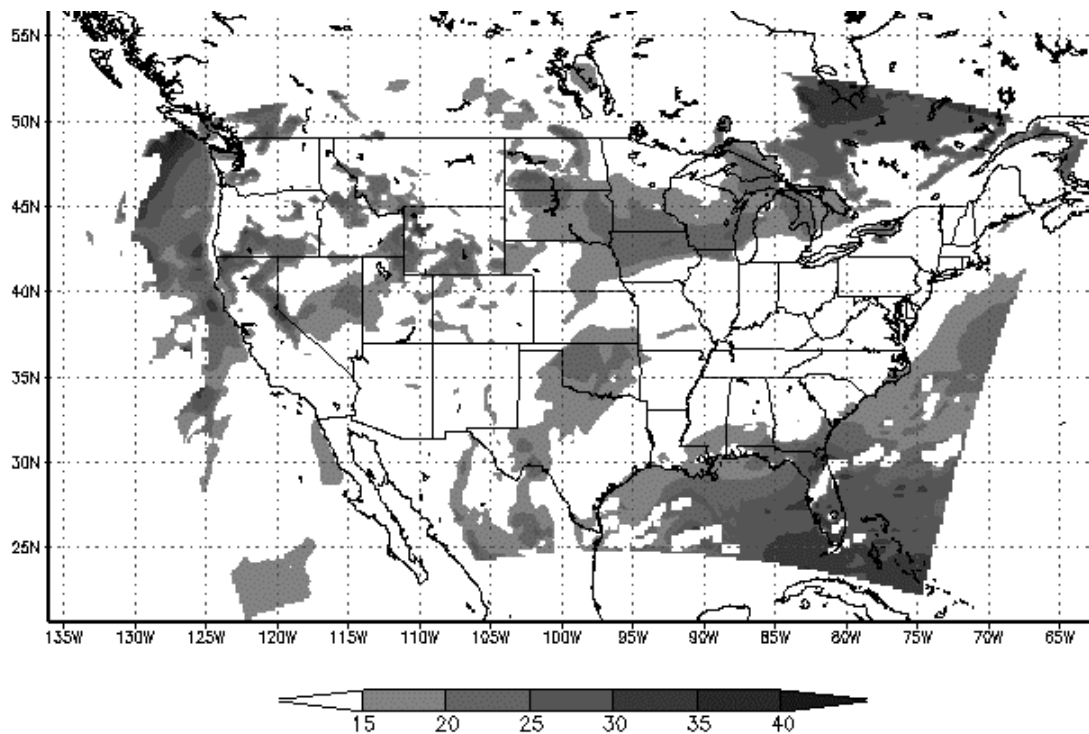


FIGURE 12. WGE Wind Gust Algorithm forecast 30 Oct 2001 valid 00 UTC. Shaded areas indicate wind gusts of at least 15 knots. Contours are every five knots.



GrADS: COLA/IGES

2002-03-08

FIGURE 13. AFWA Wind Gust Algorithm forecast valid same as Figure 12. Shaded areas indicate wind gusts of at least 15 knots. Compared to Figure 12, the AFWA algorithm is over-forecasting gust extent in OK, IA, and WI. The methods agree better off the coasts.

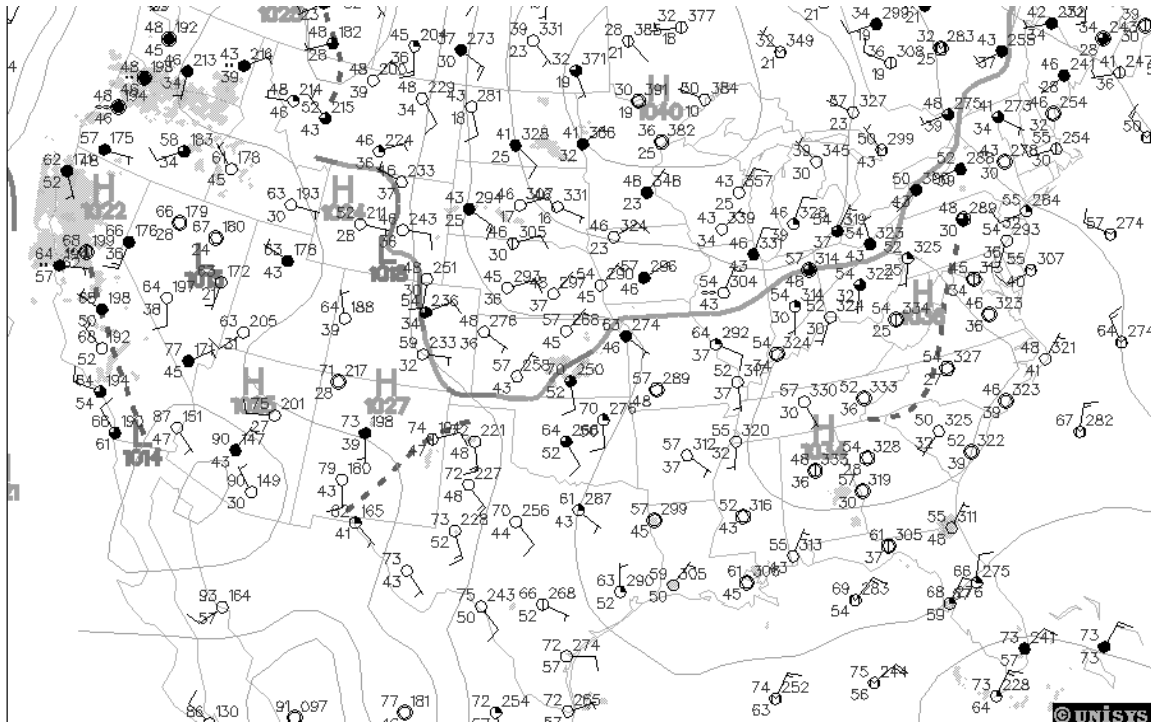


Figure 14. Synoptic map of CONUS valid at 00 UTC 30 Oct 2001. A cold front stretches from the Canadian Maritimes across the Midwest into the Central Plains. High pressure sits along the MN and Canadian border. (Adapted from Unisys 2002)

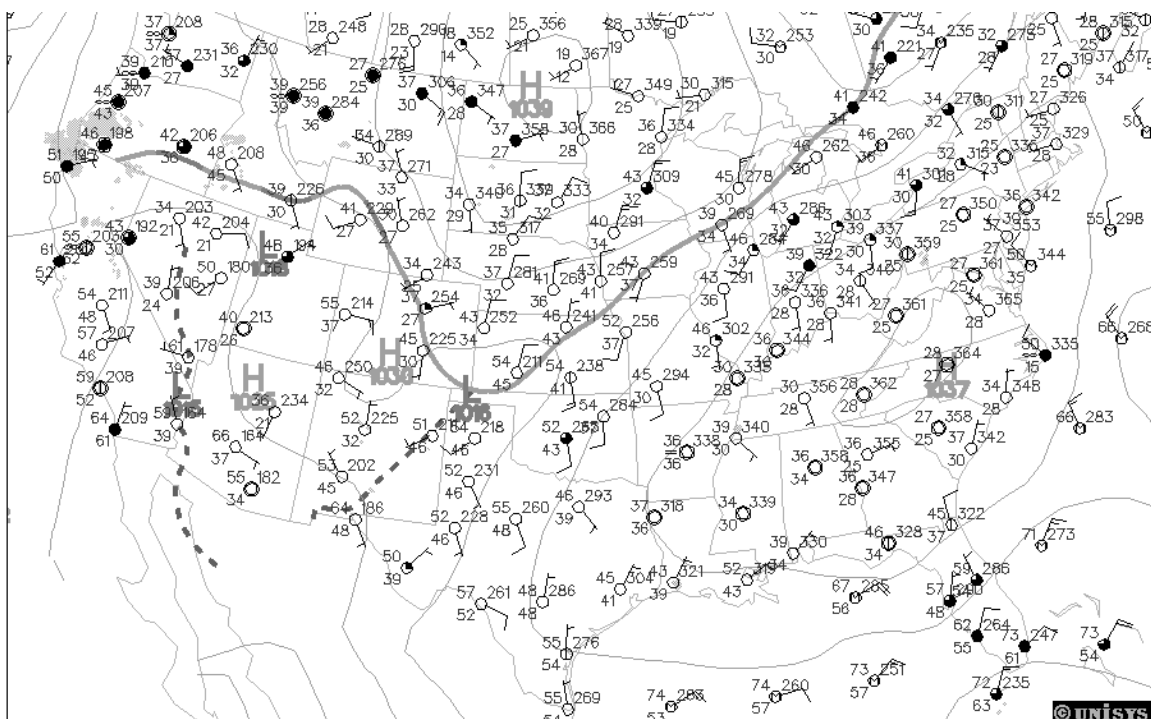


Figure 15. 12 UTC 29 Oct 2001 Synoptic Weather Map. High pressure is over ND and NC. The cold front stretches from Ontario southwest to the TX, OK panhandle region. (Adapted from Unisys 2002)

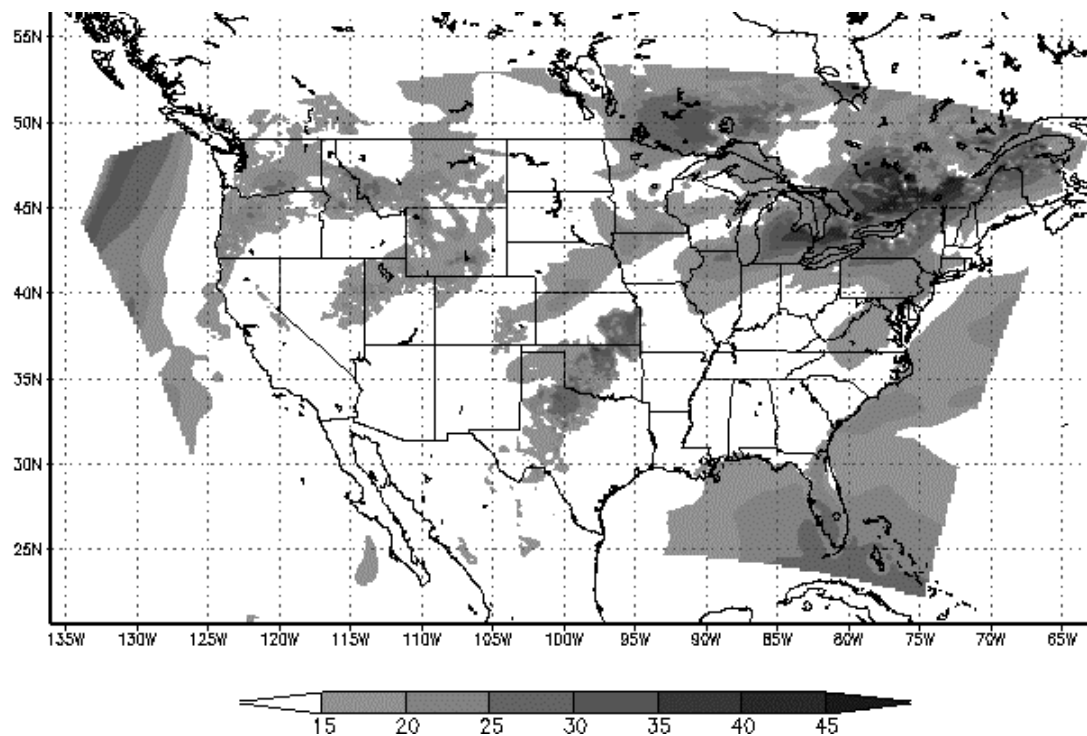


FIGURE 16. WGE Wind Gust Algorithm forecast valid 12 UTC 29 Oct 2001. Compared to Figure 12, the area extent of gusts are increased. Areas directly along the cold front are shown as non-gusty. New England still shows over-forecasting due to the nighttime. (Units kts.)

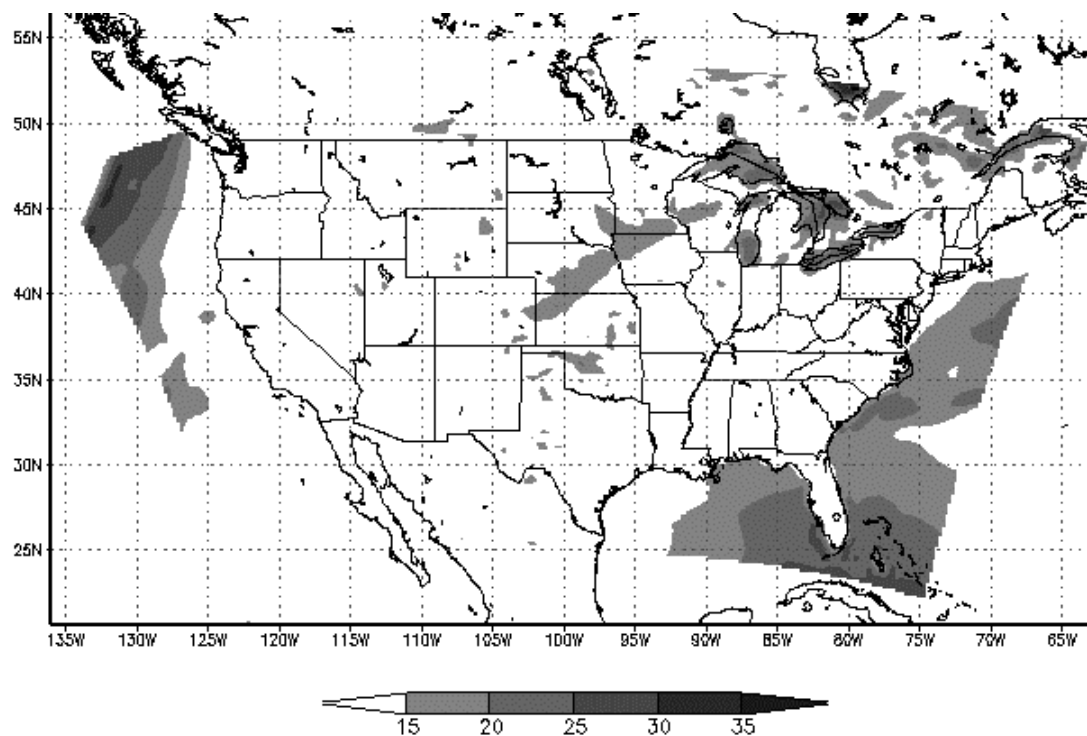


FIGURE 17. AFWA Wind Gust Algorithm valid same as Figure 16. A dramatic difference compared to Figure 16. The gusty areas show gusty winds over the Great Lakes and a small area behind the front. (Units kts).

In contrast, Figure 16 shows the difference that the time of forecast makes to the results of the WGE wind gust algorithm. The regional extent of the over-forecasting is obvious for nighttime forecasts of the WGE. Figure 17 occurs at the same forecast time but is for the AFWA algorithm. The WGE shows a marked increase in the coverage of gusty winds, especially in the northeastern and midwestern United States, as compared to Figure 12. The forecast for Figures 16 and 17 have the same initialization time, and are 18 hours earlier than those of Figures 12 and 13. The frontal system has not moved very much from its previous position, but the high over North Carolina has weakened while the high pressure over North Dakota has strengthened and advected eastward.

The WGE over-forecasts at night and where mechanical turbulence is affecting the calculation of TKE. The AFWA algorithm is over-forecasting slightly in the daytime, especially where daytime heating is the strongest, near mountain peaks, and near sunny surfaces behind cold fronts. In the daytime the over-forecasting by the WGE is decreased substantially. Mechanical turbulence near the cold front is affecting the forecast in the North East, but overall the forecasts of wind gusts are verifying well especially at stations like KRCA and KHIF (Figure 12). The AFWA algorithm in Figure 17 shows that forecasting in stable conditions at night in the presence of a weak cold front does not hinder its ability to forecast the gusty winds. In fact, this time period is especially indicative of the lack of over-forecasting by the AFWA algorithm at night. Valid times of 00 UTC and 12 UTC are the last times before the change in category from day to night. This allows the algorithms to have the maximum time to adjust to the diurnal changes of the ABL, for example the value of the SL inversion or the dissipation of TKE in the Residual Layer. When the algorithm is in its optimum time period of forecasting,

which is during the day for the WGE and at night for AFWA, it is safe to say that one algorithm is better than the other algorithm. This is borne out by comparisons to the observations at the verification stations at the time periods shown, and by the skill scores for the stations during these periods of the day. When active weather systems are near, both models will have trouble accurately predicting the wind gust.

Figure 5 showed three circled regional areas. They were classified into the coastal, mountainous and plains zones. The coastal zones consisted of stations located along the Gulf of Mexico and the Atlantic Ocean. KEYW, KCOF, KHRT, KILM, and KCRP made up the coastal stations. The mountainous region had stations near significant terrain changes. They were KMOU, KCOS, KHIF, KLSV, and KDMA. Finally the plains zone included KFFO, KBLV, KRDR, KRCA, and KICT, all of which are located in or near the Great Plains. The regions were broken out of the total station list to help identify any regional differences in the scores of the WGE and AFWA wind gust algorithms. The mountainous zone did not pass the Fisher-Irwin Exact Test for sufficient time periods to have the results plotted. The alpha was 0.05, and indicates that the results are not significant to the total results from the combined stations.

In Figure 18 the differences between the two algorithms for values of CSI, POD and FAR are shown. The CSI and POD differences are calculated by subtracting the value of the WGE algorithm score from the AFWA score. FAR has a negative response so it is calculated by subtracting the WGE score from the AFWA value. This means all values above zero indicate WGE out-performance of the AFWA gust algorithm. Less than zero indicates the AFWA algorithm is better. Figure 18 shows that WGE algorithm sometimes outperformed the AFWA algorithm in CSI and FAR. POD was much lower

for the WGE in almost all time periods. Figure 19 shows the reverse of Figure 18, with the AFWA algorithm significantly outperforming the WGE algorithm in the plain zone. The values of the average categorical scores in the coastal zone for the WGE, and the plain zone for the AFWA algorithms, prove there are geographical regions that are sensitive to the algorithms. In the coastal zone if one method must be chosen, pick the WGE. In the plains, choose the AFWA algorithm.

The Bias scores of the regions show the most significant results from the regional breakdown. Figures 20 and 21 show the coastal and plain zones comparative Bias scores respectively. The mountainous regions are not shown because the scores may not be reliable, but they typically over-forecasted the most of all regions. Results showed the WGE method was over-forecasting as much as seven times what was observed in the mountain zone. Both algorithms tended to over-forecast at night.

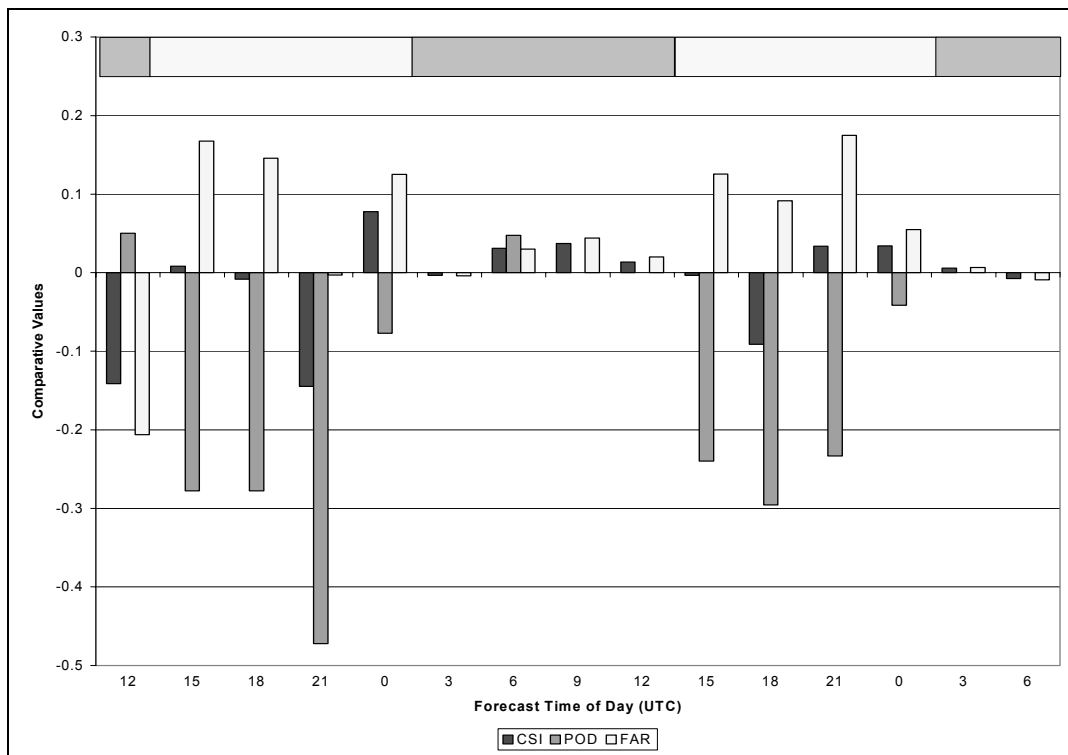


FIGURE 18. Differencing of WGE and AFWA Coastal Zone Stations Categorical Scores at 06 UTC. Positive values indicate scores where the WGE method is better.

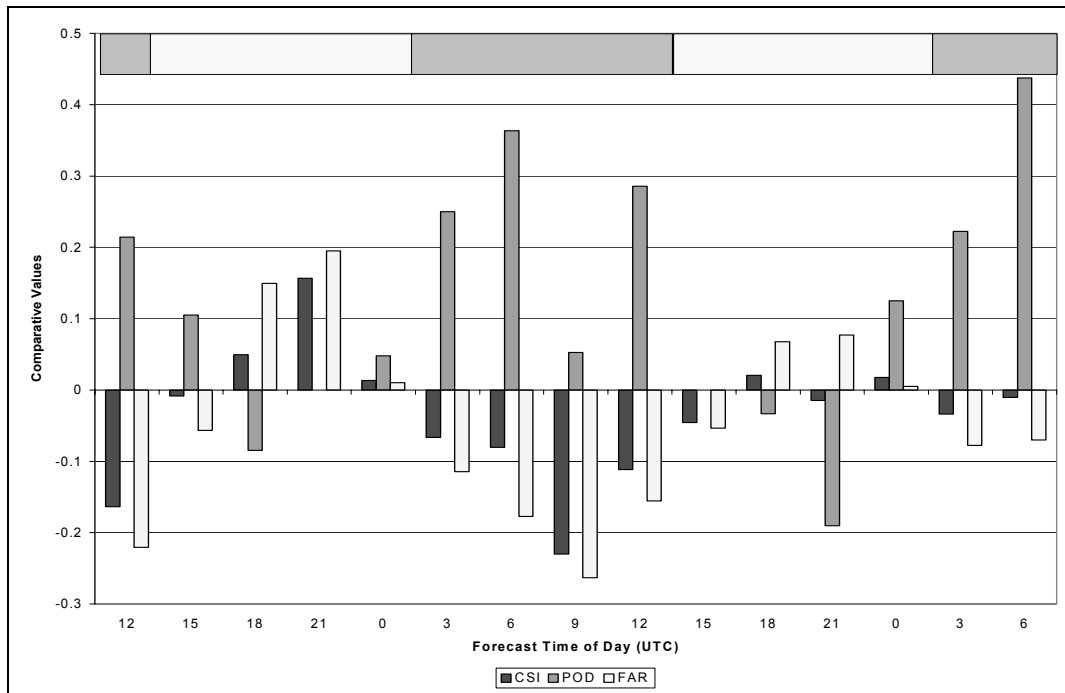


FIGURE 19. Differencing of WGE and AFWA Plain Zone Stations Categorical Scores at 06 UTC. Negative values indicate scores when the AFWA method is better. A diurnal trend is noticeable, but the AFWA algorithm scores better the WGE algorithm.

The comparisons of skill scores are shown in Figures 22 and 23. The coastal zone stations are shown in Figure 22, and the plains stations are displayed in Figure 23. Again the mountainous stations did not have the necessary significance to display the results. Figure 22 shows that the skill of the WGE method is much better at most times over the AFWA algorithm, and can be said to outperform the AFWA method. The plain zone shows the reverse in the skill scores. The AFWA method is better, and is outperforming the WGE in categorical skill scores.

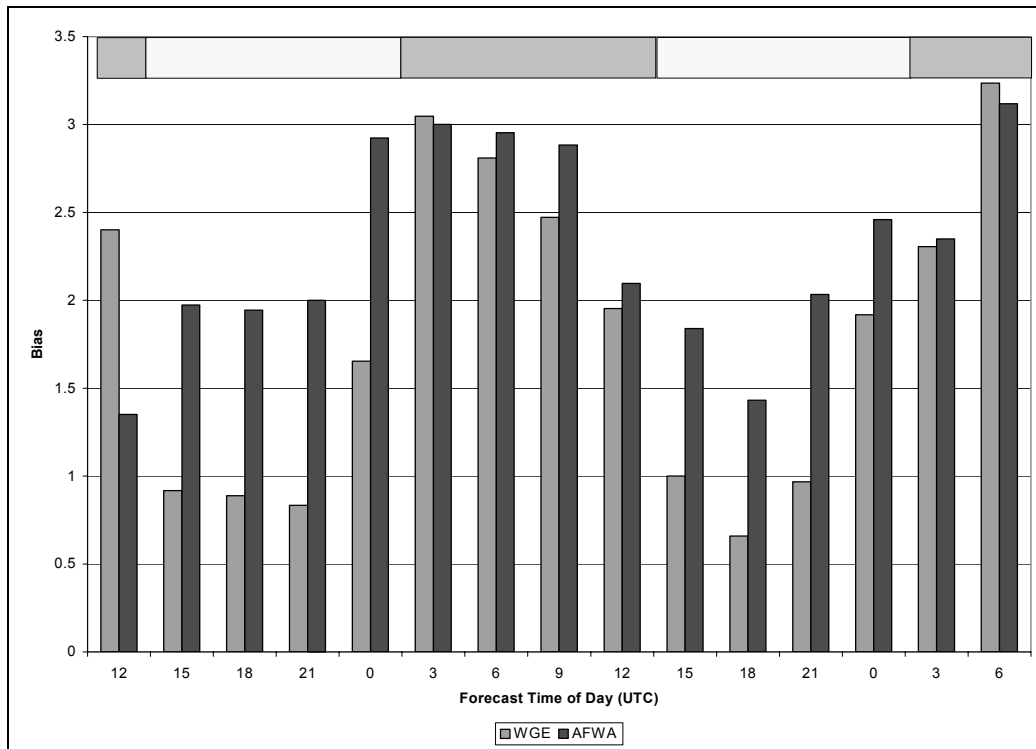


Figure 20. Comparison of the Bias of the WGE and AFWA Coastal Zone Stations 06 UTC. The Bias values are significantly lower than the Bias scores for all 06 UTC run sites.

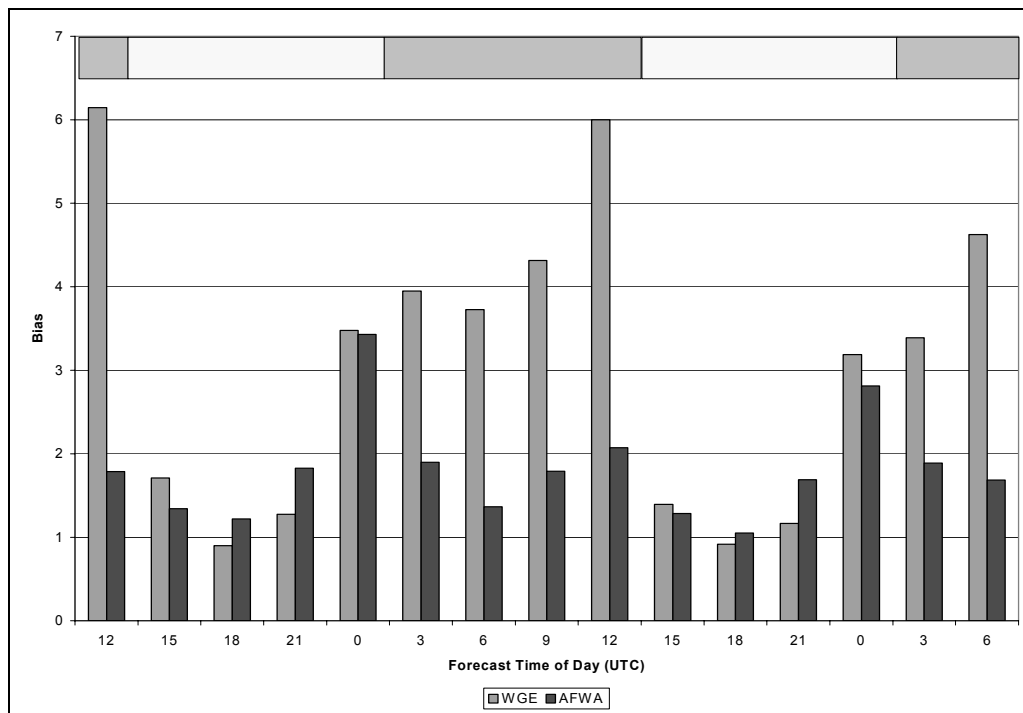


FIGURE 21. Bias Scores for the WGE and AFWA Algorithms Plains Zone Stations 06 UTC. The Highest level of WGE Bias occurs at the later nighttime periods. The AFWA Bias is generally very low.

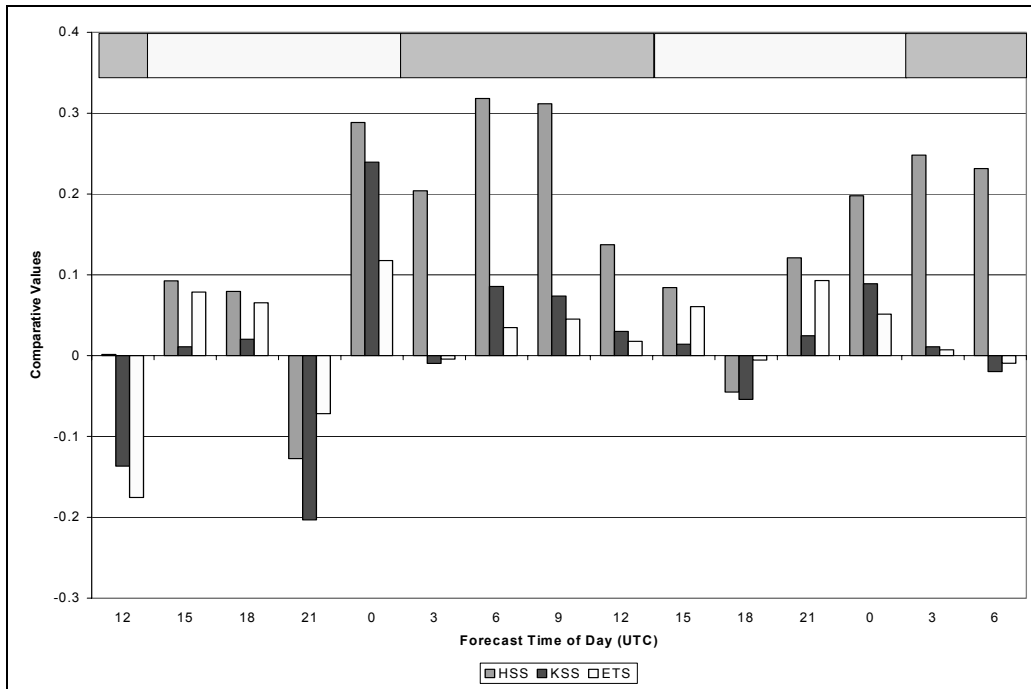


FIGURE 22. Differences of Skill Scores WGE-AFWA Coastal Zone Stations 06 UTC. The WGE shows definite improvement over the AFWA algorithm in almost all forecast periods.

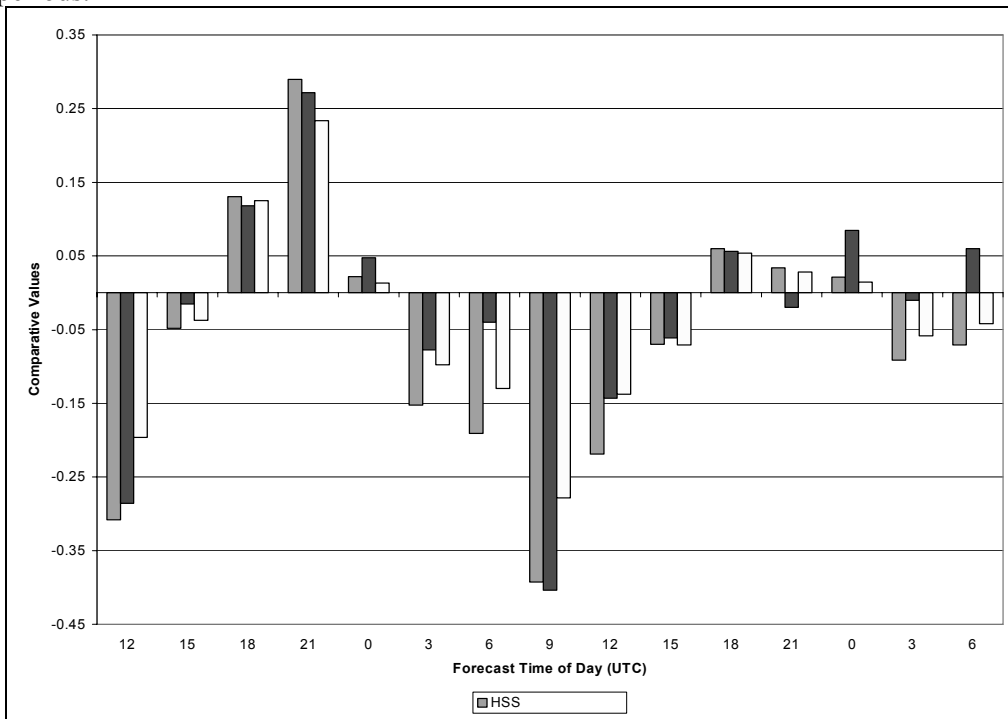


FIGURE 23. Differences of Skill Scores WGE-AFWA Plain Zone Stations 06 UTC. The AFWA algorithm is better for most time periods. The daytime periods the WGE has some skill still, and early in the forecast, does moderately well against the AFWA method.

4.4 18 UTC AFWA MM5 Model Run

Results from the 18 UTC run of the AFWA MM5 model run show the same diurnal patterns of WGE and AFWA wind gusts as in the 06 UTC runs. The AFWA model generally scored better in the skill scores than in the 06 UTC runs. A possible explanation for this result is because there are eight nighttime periods in the 18 UTC run and only seven in the 06 UTC run. The daylight periods for the 18 UTC run are the 6-, 21-, 24-, 27-, 30-, 45-, and 48-hour forecast periods. The verification of the data was accomplished the same way as in the 06 UTC run, with two-by-two matrices calculated on all fifteen forecast periods. Appendix C lists the forecast times and gives the data for each forecast period of the 18 UTC run.

The 18 UTC run showed the same trend as before, especially in the Bias, for the WGE to over-forecast during the nighttime hours. This time the average values of the skill assessments showed the AFWA algorithm to be more closely matched to the WGE algorithm. Once again the Bias of both algorithm's 15, 18, 21 and 00 UTC forecast times are much less than those of the 03, 06, 09 and 12 UTC times. The WGE and AFWA algorithms show the same diurnal time dependence, with an increase in over-forecasting in the nighttime hours (Figure 24-26). The AFWA value is likely an aberration because it is under-forecasting the winds at the same time. The 6-hour 18 UTC forecast period is the only time that the AFWA algorithm under-forecasts wind gusts for either the 06 or 18 UTC run times. A possible explanation for the poor performance of the WGE at the 6-hour forecast time is the extremely high FAR for the WGE. The FAR is 0.756 compared to 0.546 for the AFWA model for the first time period. The average daytime FAR for the WGE is 0.515 neglecting the first time period.

This indicates many “yes” forecasts and not many corresponding “yes” observations.

The following figures show the comparative or difference values of the WGE and AFWA algorithms two-by-two scores (Figures 24-26). The figures were computed the same as for the 06 UTC run.

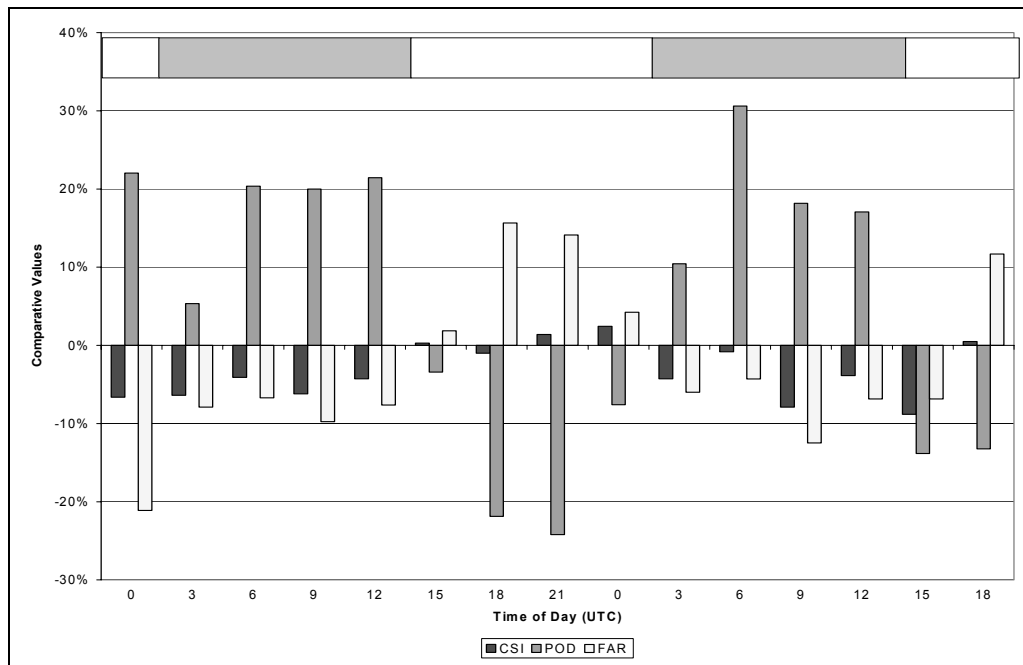


FIGURE 24. Differences of Categorical Scores WGE-AFWA for the 18 UTC run. Positive values indicate the WGE performed better than the AFWA algorithm.

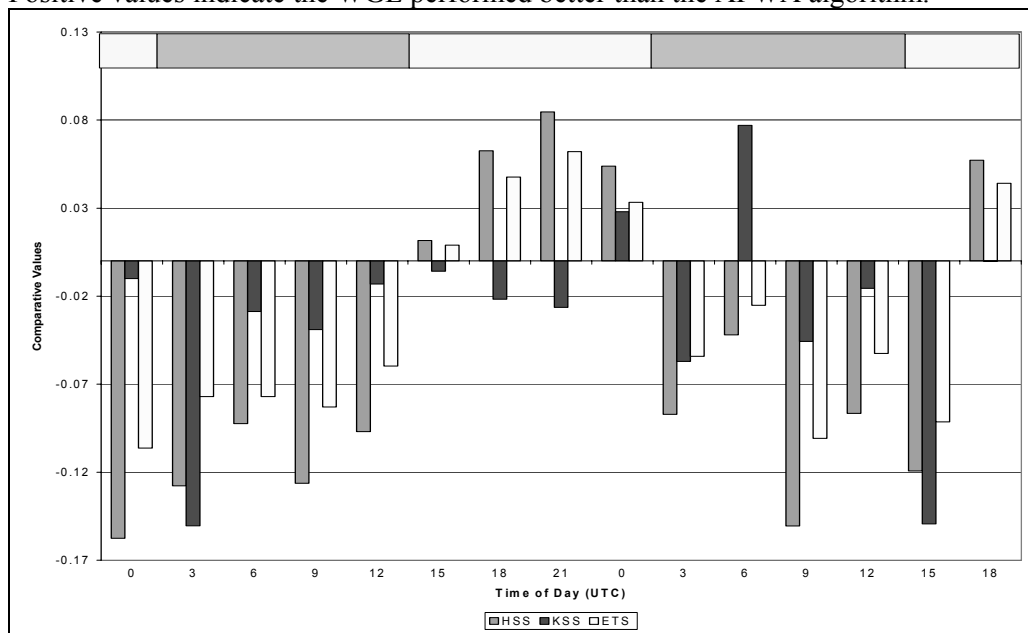


FIGURE 25. Differences of WGE-AFWA Skill Scores 18 UTC Run. The diurnal tendency of the algorithm’s scoring is apparent in this graph.

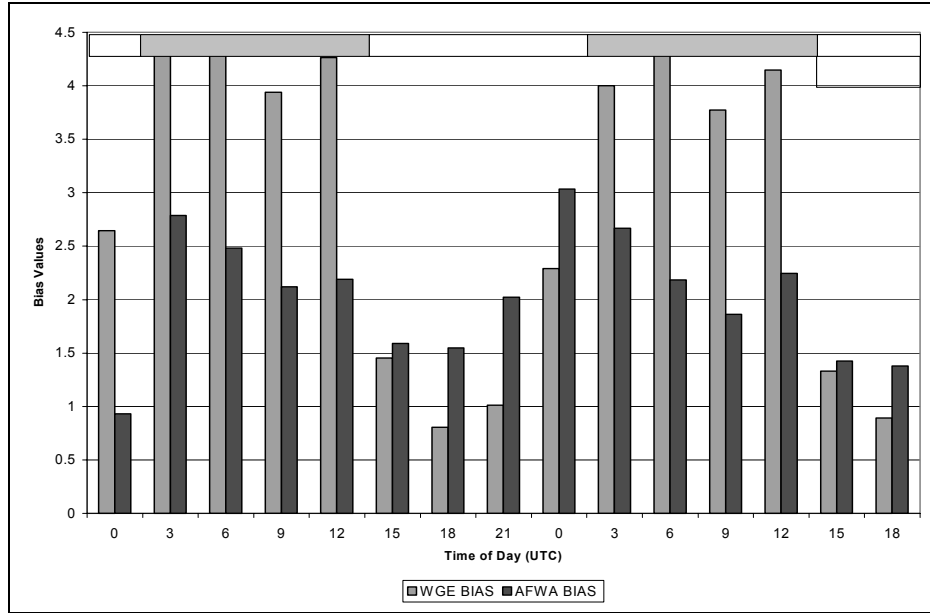


FIGURE 26. Comparison of the Bias between the WGE and AFWA algorithms 18 UTC run. The nighttime hours show a significant over-forecasting of wind gusts by the WGE. The first forecast time period shows that despite the daylight time period the WGE Bias is greater than the AFWA algorithm.

The Bias of the AFWA gust algorithm shows that it has a problem with over-forecasting during the nighttime hours, similar to the Bias scores of the WGE. Table 8 and Table 9 list the two-by-two table scores. The differences are computed the same as in Table 6.

TABLE 8. The 18 UTC Run Mean 2X2 Scores

	WGE	AFWA	
	raw score		difference
Hit Rate:	0.668	0.748	-0.080
CSI:	0.251	0.284	-0.033
POD:	0.699	0.645	0.054
FAR:	0.686	0.658	0.028
BIAS:	2.908	2.031	0.877

TABLE 9. The 18 UTC Run Mean Skill Scores

	WGE	AFWA	
	raw score		difference
HSS:	0.241	0.296	-0.055
KSS:	0.376	0.406	-0.031
ETS:	0.141	0.176	-0.035

For the 18 UTC run the WGE fails to beat the AFWA algorithm in any skill score in an aggregate fashion (Table 9). Figure 25 indicates the WGE algorithm is better in the middle daylight periods. The FAR is also worse for the WGE (Figure 24) than the AFWA wind gust algorithm, however, a time comparison of the data shows that the FAR is better for the WGE than the AFWA during the daylight hours. The AFWA FAR never drops below 50 percent, while the FAR drops below 40 percent twice for the WGE. The average POD shows that the WGE is better than the AFWA algorithm by better than 5 percent.

Figures 27 through 30 are maps similar the 06 UTC run maps. They are showing the general over-forecasting that a particular method has based upon the time of day. The WGE generally over-forecasts at night, and the AFWA algorithm over-forecasts in the day. The difference in the over-forecasting is noticeable: the AFWA algorithm does not over-forecast in the day as badly as the WGE does at night. It should be noted that the AFWA algorithm is also over-forecasting at night along with the WGE method. Figure 27 shows the WGE method in the daytime when it has a reasonable forecast based upon verification from the gust that occurred at the stations, and the coverage of gusts. Figure 28 is the AFWA gust for the same time, 21 UTC 8 November 2001. Figures 29 and 30 are nighttime forecast wind gust pictures valid at 09 UTC 22 October 2001. Figure 29 is the WGE method and Figure 30 is the AFWA method. The amount of over-forecasting by the WGE method is apparent in Figure 29.

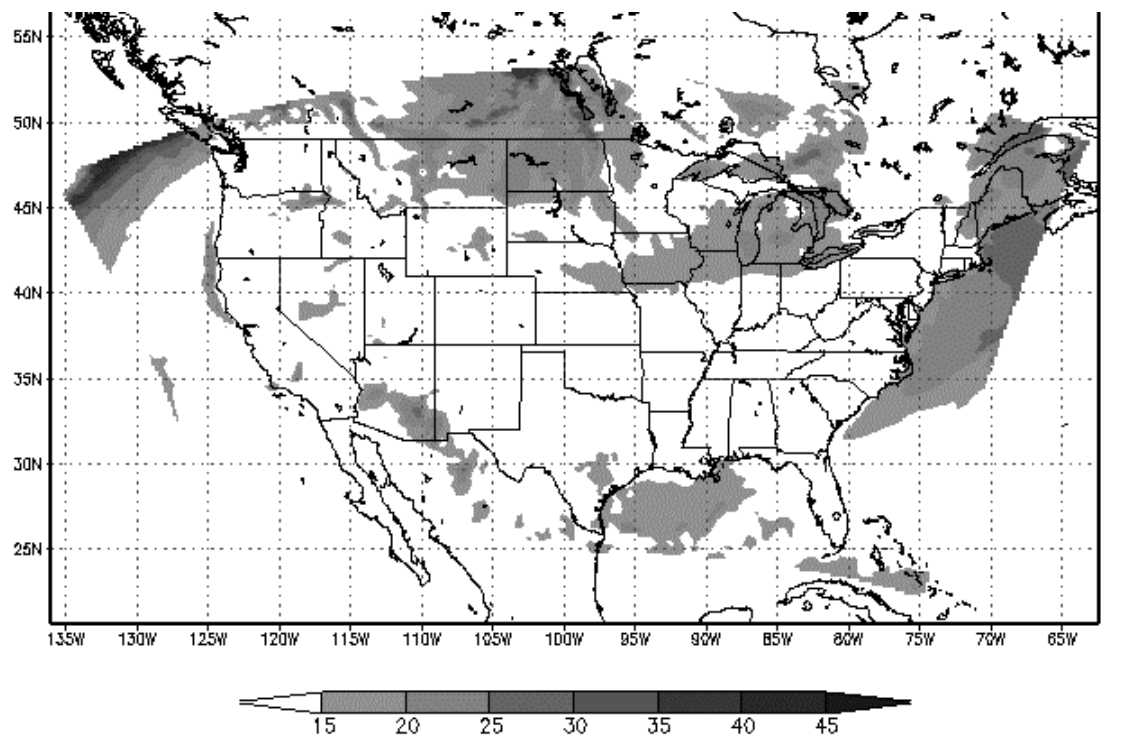


FIGURE 27. WGE Wind Gust Forecast Valid 21 UTC 8 November 2001. A cold front is moving south from the Canadian Great Plains, and a Low is centered to the northeast of MI. (Units kts).

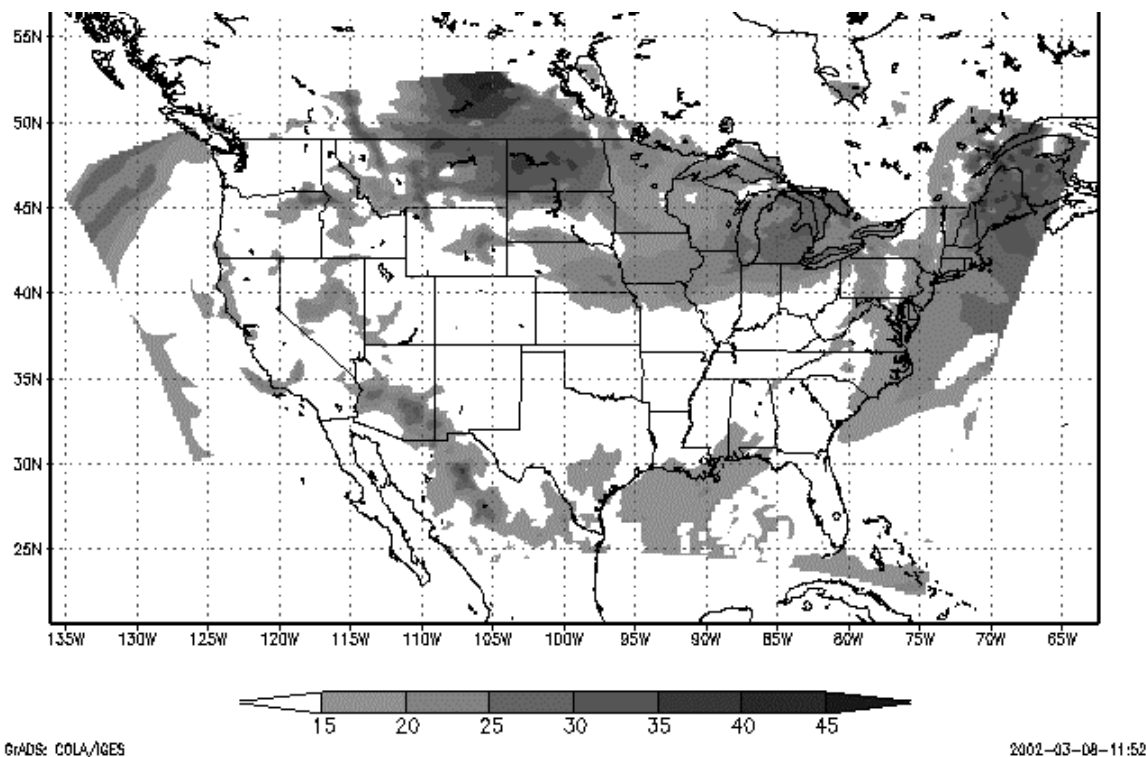


FIGURE 28. AFWA Wind Gust Forecast Valid 21 UTC 8 November 2001. Over-forecasts for central MN and upper WI. Values of gusts are unrealistic over ND. (Units kts).

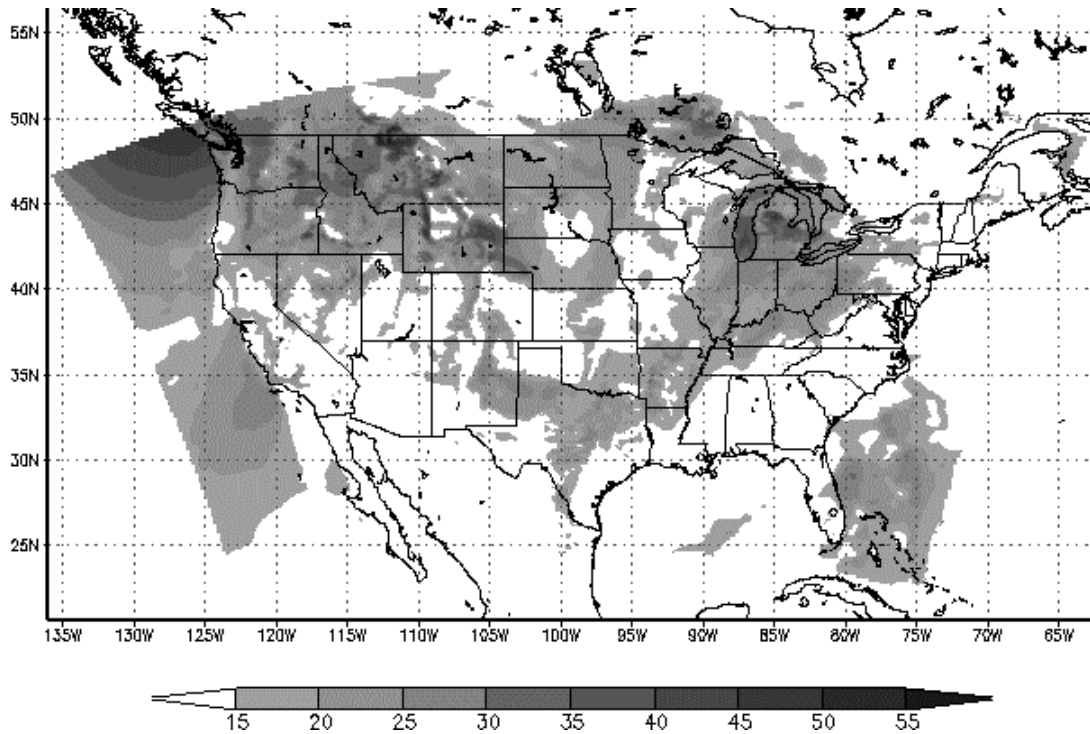


FIGURE 29. WGE Wind Gust Forecast Valid 09 UTC 22 October 2001. Major over-forecasting of the algorithm this forecast time. Frontal system stretched from Ontario to TX, OK panhandle. This is the nighttime over-forecasting typical for the WGE. (Units kts).

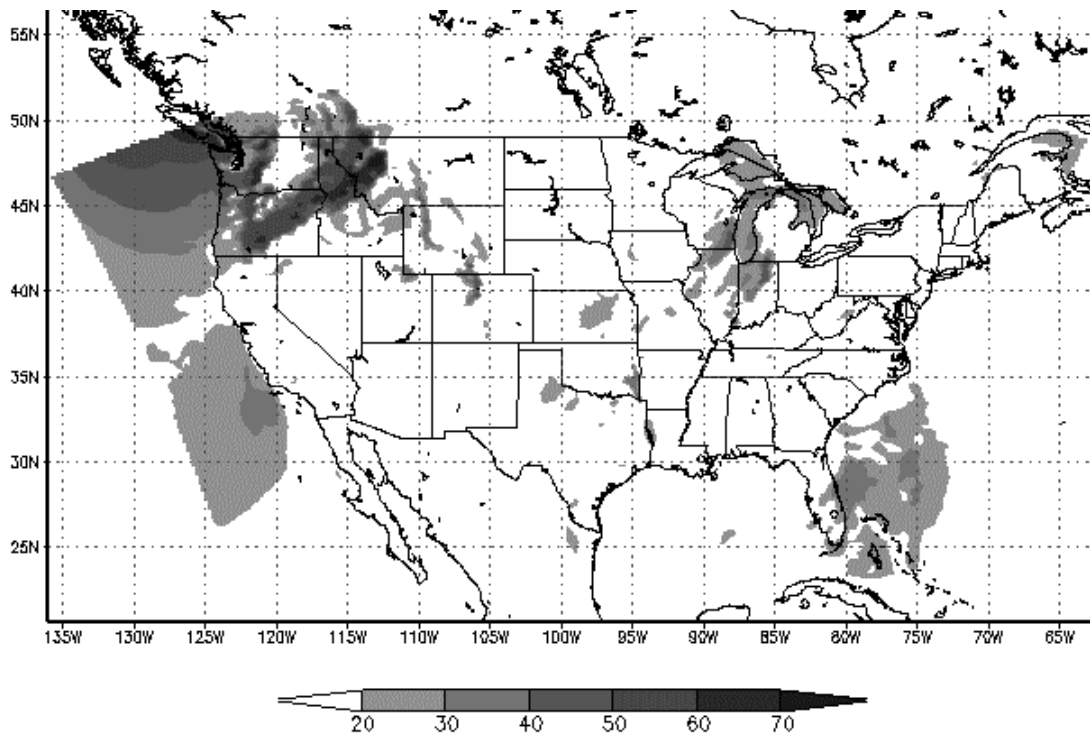


FIGURE 30. AFWA Wind Gust Forecast Valid 09 UTC 22 October 2001. The same forecast time as in the Figure 29, the AFWA algorithm is better than the WGE by looking at gusty area coverage. Contours every 10 knots.

Geographical zone differences between the two algorithms are similar to the 06 UTC run results. Comparing and differencing categorical scores between the WGE and AFWA algorithms show that the diurnal trend identified in previous 18 UTC graphs continue with the 18 UTC geographical zones (Figures 24-26). The zones are the same as in the 06 UTC run. Figures 31 and 32 show the comparative scores of the coastal and plain zones. Figures 33 and 34 show the skill scores comparatively for the coastal and plain zones. Figures 35 and 36 show the Bias scores. The same Fisher-Irwin Exact test for significance was accomplished on the two-by-two scores. Only the mountainous zone stations had any stations that failed to satisfy the test for independence at a level of 0.05. Values above zero are indicating the WGE performed better in that statistic, while negative numbers show worse results for the WGE method.

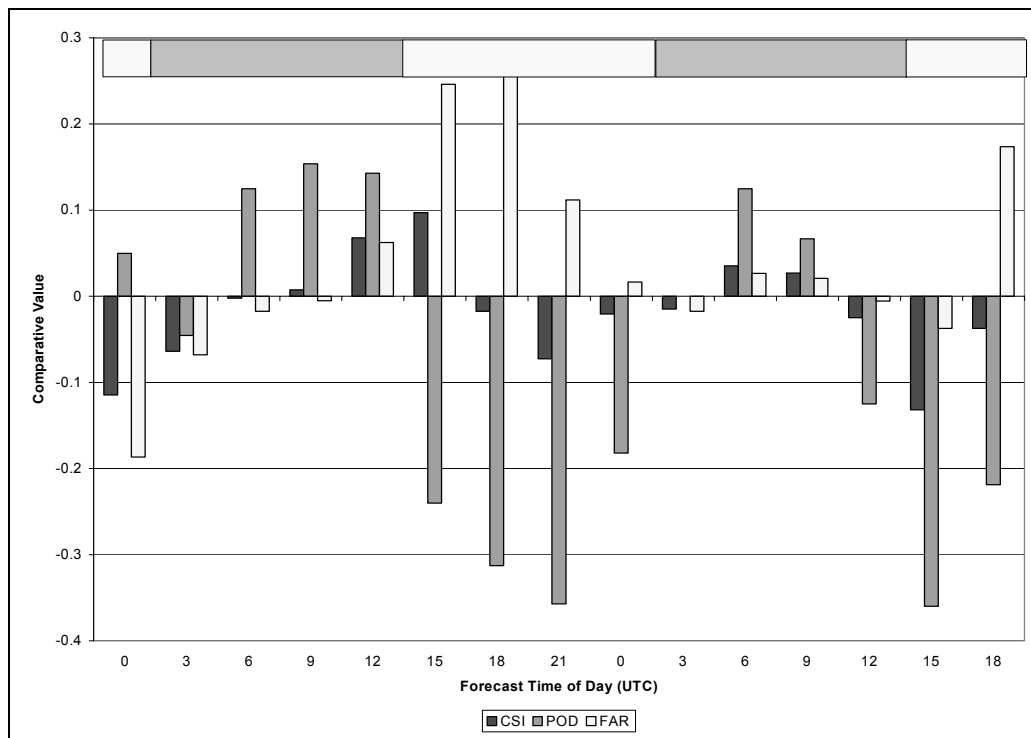


FIGURE 31. Differences in Categorical Scores WGE-AFWA Gust Algorithms Coastal Zone Stations 18 UTC Run. The WGE is better than the AFWA method at night.

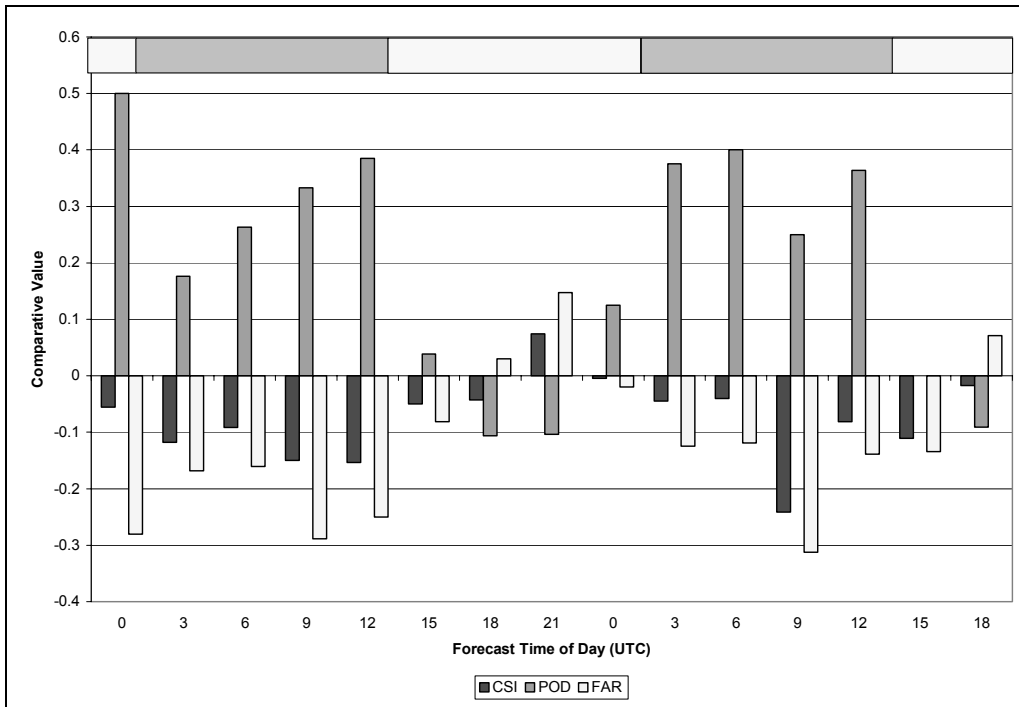


FIGURE 32. Differences in Categorical Scores WGE-AFWA Gust Algorithms Plain Zone Stations 18 UTC Run. AFWA algorithm has better scores at night.

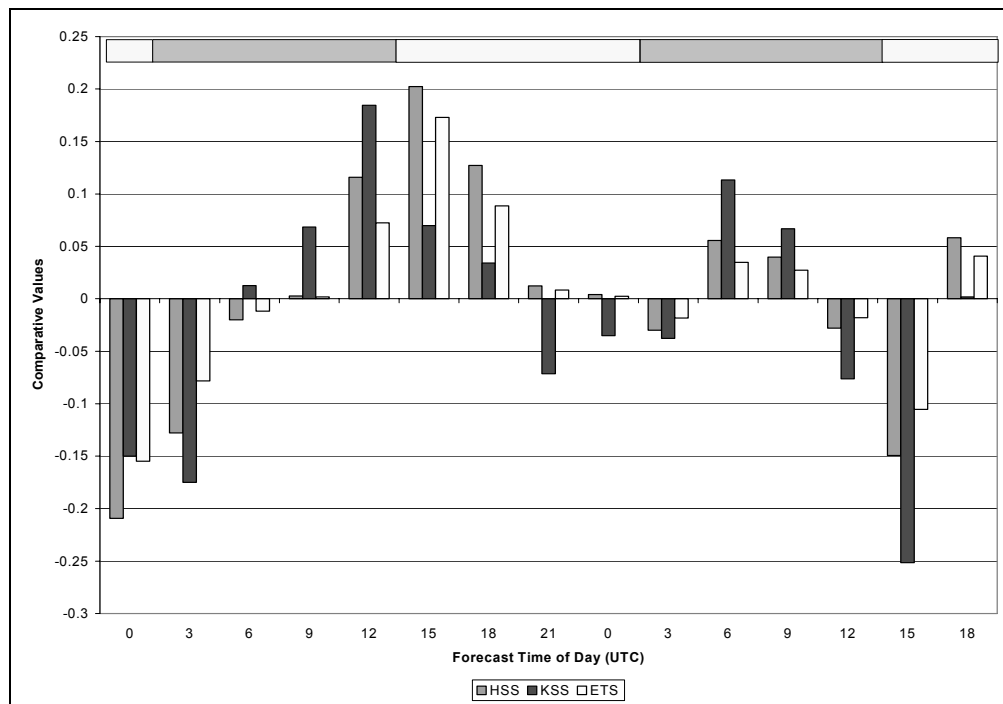


FIGURE 33. Differences in Categorical Scores WGE-AFWA Gust Algorithms Coastal Zone Stations 18 UTC Run. The typical diurnal patterns are not evident in this graph.

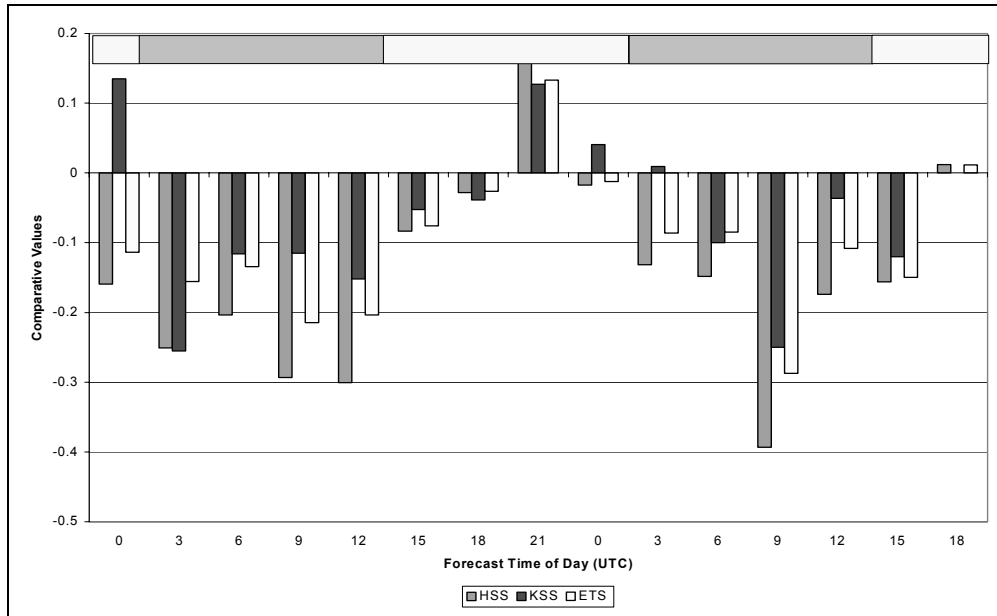


FIGURE 34. Differences in Skill Scores WGE-AFWA Values Plain Zone Stations 18 UTC Run. The low scores of the WGE in the plains are shown in this graph. The AFWA model betters the new WGE in all but one daylight period.

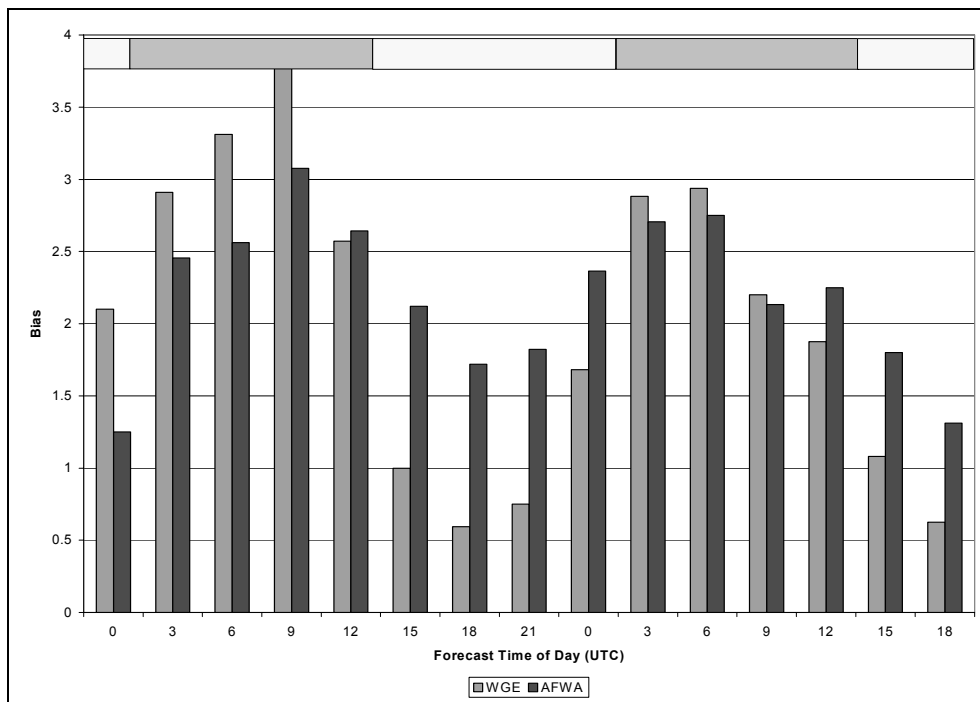


FIGURE 35. Comparison of the WGE and AFWA Bias for the Coastal Zone Stations 18 UTC Run.

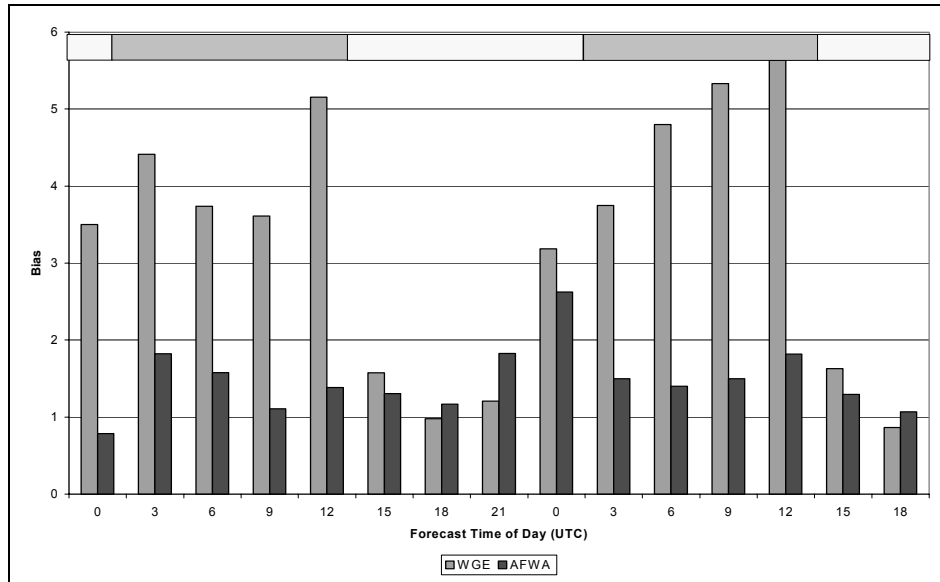


FIGURE 36. Comparison of the WGE and AFWA Bias for the Plain Zone Stations 18 UTC Run. The WGE is over-forecasting for almost all time periods. Only the central daytime periods does the WGE perform better than the AFWA algorithm. Daytime values are generally good for both models.

Analyzing the different zones for patterns, it becomes obvious that 18 UTC results from the plain zone stations are similar to the results from the 06 UTC plain zone stations. The AFWA algorithm is generally forecasting very well, and not really over-forecasting at any time period as in Figure 36. The skill scores of the AFWA plain stations show it is scoring better in Skill Scores (Figure 34) and raw categorical scores (Figure 32.) For the coastal zone stations no conclusion can be made about the best time of day for one of the methods. The usual diurnal pattern is skewed as is evident in Figure 33. The skill scores show that there is not a preferred time of day for the WGE method. Figure 31 shows that the WGE is generally performing better at night, and worse in the day.

4.5 Quantitative Comparison of the WGE and AFWA Wind Gust Algorithms

In addition to the categorical assessment of the relative qualities of the WGE and AFWA wind gust algorithms, a numerical assessment of the strengths and weakness of the two was accomplished. When a wind gust was actually observed, the forecasted value was quantitatively evaluated. Figure 37 shows results from the 06 UTC run of the MM5 and the RMSE in knots, and Figure 38 depicts results from the 18 UTC run.

The data indicate that if a gust occurs then the WGE is more accurate than the AFWA gust algorithm. When the number of observations that contain a gust increases, the RMSE difference between the two algorithms is less noticeable. Figures 37 and 38 show that the WGE is better overall than the AFWA algorithm by having lower RMSE error. The greatest improvement in the WGE gust forecast occurs during the nighttime hours. This might indicate that the WGE method of computing gusts is legitimate, because the WGE is looking for the maximum value in a critical layer, while the AFWA method uses the average wind in the surface layer for computation of the non-convective winds. The WGE method is going to forecast many more gusts than actually occur, but when the gust does occur it is accurate.

When looking at a single station, for all observations containing a gust, the RMSE results show that the WGE performs better than the AFWA algorithm. Chosen at random from the remaining stations not analyzed in the geographical regions, Richmond, VA (KRIC), shows the WGE performs better at almost all time periods when a gust occurred. Figure 39 shows the value of the algorithm minus the observed gust for both algorithms.

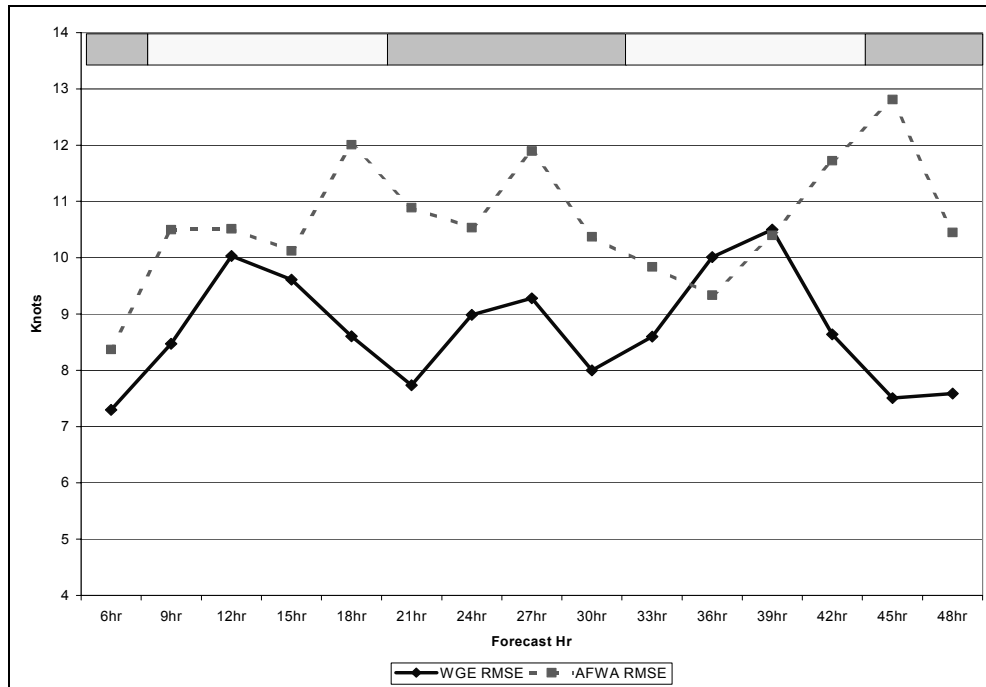


FIGURE 37. 06 UTC Quantitative Comparison of the WGE and AFWA Wind Gust Algorithms. Forecast hour is on the bottom axis, and RMSE error in knots along the vertical axis. The WGE shows better performance than the AFWA for all but two time periods.

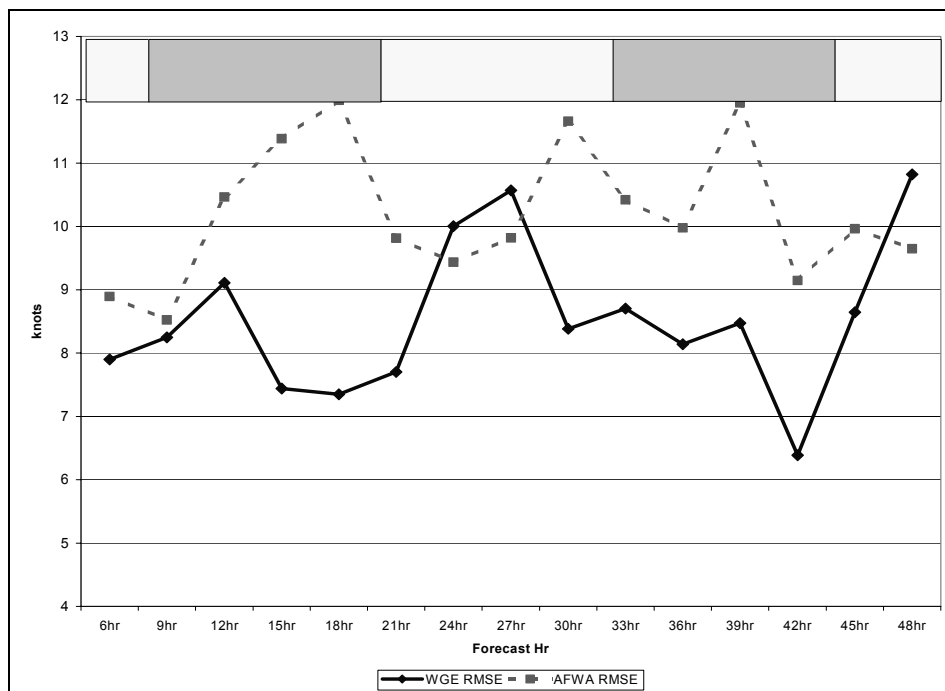


FIGURE 38. 18 UTC Quantitative Comparison of the WGE and AFWA methods. The WGE is still overall a better performer for all but three time periods.

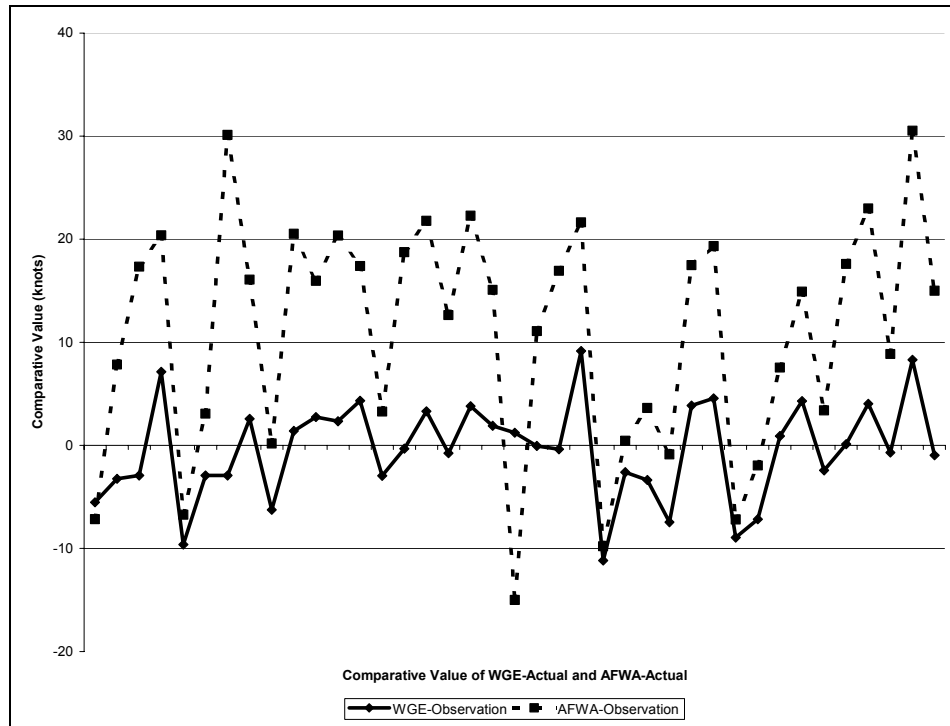


FIGURE 39. Comparison of the (WGE forecast – observation) values and the (AFWA forecast – observation) for 06 UTC KRIC gusts. A score of zero is a perfect forecast. When a gust occurred, the corresponding forecast was subtracted from the observed gust. The AFWA algorithm shows a great over-forecasting of the wind gust. The WGE indicates an accurate representation of the winds, and is better than the AFWA algorithm.

V. Conclusions

This research shows several key results relating to the WGE wind gust algorithm used and the AFWA wind gust algorithm. Many of the items can be traced to the diurnal variation shown by both gust algorithms. This research does show that improvement can be made towards a better wind gust forecast algorithm for the AFWA and Air Force meteorologists.

5.1 Summary of Results

The most obvious result from this research is that the WGE algorithm categorical scores are better in the daytime than in the nighttime as compared to AFWA algorithm categorical scores. For all the stations, CSI and FAR from both the 06 and 18 UTC runs were generally better for the WGE algorithm. Conversely, the 03, 06, 09, and 12 UTC forecasts showed the AFWA algorithm scored better. Skill scores for both algorithms showed the same trends as the CSI and FAR scores.

The greatest indication of the swing in diurnal performance of the algorithms was shown in the Bias scores of the two algorithms. The nighttime Bias scores of the WGE algorithm indicate the WGE method over-forecasted at night for almost all periods. The AFWA method showed that it too over-forecasted at nighttime, but not to the same degree as the WGE method. In the daytime, the WGE Bias scores were close to one, which is a perfect forecast, while the AFWA method continued to over-forecast. This over-forecasting by the algorithms helped explain the differences in the POD and FAR scores. The algorithm that tended to over-forecast at a specific time generally had a higher POD score at that time. For daytime scores the over-forecasting AFWA algorithm

had better POD scores. At night, the WGE method hardly missed any gusts because of its over-forecasting tendencies. Along with scoring higher POD rates, the FAR rates were also higher. Whichever method was over-forecasting had the higher FAR. Operational forecasters using this data need to consider both scores when weighing which method to use.

The geographical breakdown of the stations showed that regional differences in the boundary layer weather affected each algorithm differently. The diurnal trend shown in the comparison using all stations was not apparent when the coastal stations were examined separately. Categorical and skill scores of the mountain zone stations were not shown because the statistical significance of the two-by-two tables was not met. However, the mountain zone stations showed continued over-forecasting of the WGE algorithm at nighttime forecast periods.

The continental interior stations as typified by the plain zone stations showed that the AFWA wind gust algorithm was superior to the WGE method in almost all forecast periods, and for almost all scores except the POD. In a reversal of the summary of the total station Bias scores, the plain zone station Bias scores for the AFWA method are generally lower at all times than those of the WGE method. Thus the SL method, which is used for AFWA's non-convective portion of the wind gust algorithm, is better in flat interior stations where the surface layer inversion is better resolved by the model.

Brasseur (2001) shows in his research on the WGE method that the comparison of the WGE method to the SL method indicated his WGE method generally performed better. His research was done in Belgium, located on the North Sea. Thus, the coastal

influence could dominate the results of his research, and he would not see the difference that the continental interior would make.

Finally, the most important result of this research is the quantitative comparison of the two algorithms. The RMSE of the WGE wind gust algorithm is better than the RMSE of the AFWA algorithm for both MM5 run times. The results show that the WGE method is calculating the gust as expected. Despite the over-forecasting of the algorithm, the WGE method is more accurate than the AFWA method.

5.2 Further Research Directions

Some of the limitations of the WGE method as implemented in this study should be resolved in future research. Brasseur (2001) believes that the TKE must be included in the model output in order to use the WGE method (Equation 6). Due to the lack of TKE data in the model output from AFWA, the ergodic assumption was made in order to estimate the TKE.

A better solution than to use the ergodic assumption is to use the TKE from the MM5. The current PBL scheme used by the MM5 run at AFWA does not produce values of TKE in the boundary layer. The Gayno-Seaman PBL scheme does produce TKE, and it would be valuable to allow this scheme to be implemented to potentially improve the gust forecasting at AFWA.

Finally, the AFWA method combines convective and non-convective wind gusts into its forecast algorithm. This study had to exclude areas where the gusts were convectively produced by the AFWA algorithm. Since most severe gusts occur from thunderstorms, it would be beneficial to have an algorithm that combines convective and

non-convective portions. Recent research (Geerts 2001) has shown that the method for convective gusts used by AFWA have been superseded by more advanced methods of convective gust forecasts. The WGE method can be easily adapted to include a convective gust forecast.

Appendix A. Statistical Analysis of Two-by-two Matrices

Two-by-two contingency tables are a routine way of assessing categorical forecasts. Several standard methods of skill scores are also used to evaluate the ability of a forecast method to improve over either random forecasts or forecasts based upon climatological standards. A two-by-two contingency table is constructed as follows;

		Event Observed		
		Yes	No	
		a	b	
Event Forecast	Yes	a	b	a+b
	No	c	d	c+d
		a+c	b+d	n

FIGURE A1. The 2x2 Forecast Verification Matrix

The value “n” represents the total number $a+b+c+d$. Along the sides and bottom are the marginal totals. Combinations of these values are used to score the two algorithms. Of these, the Air Force Weather Agency routinely uses the Critical Success Index, Probability of Detection, and the False Alarm Rate to score the MM5 model forecasts.

The various methods of scoring the two-by-two contingency tables are (Wilks 1995):

The Hit Rate (HR) is a measure of correct yes and correct no forecasts over the total number. A perfect forecast will have a Hit Rate of 1. Given by:

$$HR=(a+d)/n \quad (A1)$$

A better measure of the accuracy of the algorithm is the Critical Success Index (CSI) (Equation A2). This is especially good for the two wind gust algorithms because wind gusts might occur only twenty five percent of the time. So therefore if yes is

forecasted infrequently, it provides a better indication of accuracy than the HR. A perfect forecast will have a CSI of one, while a total failure will have a score of zero.

$$CSI=a/(a+b+c) \quad (A2)$$

Probability of Detection (POD) is a measure of detecting the yes observations. It represents the likelihood of a wind gust occurring when forecasted to occur. A POD of 1 is a perfect forecast.

$$POD=a/(a+c) \quad (A3)$$

False Alarm Rate (FAR) relates gusts that fail to occur despite the fact they were forecasted to occur. A perfect forecast will have a FAR of zero.

$$FAR=b/(a+b) \quad (A4)$$

Bias is the degree of correspondence between the average yes forecasts and the average yes observations. The Bias does not define any accuracy of the forecast, it determines if the algorithm is over or under-forecasting the wind gusts. A Bias of 1 is a perfect forecast. Values of Bias over one indicate over-forecasting, while values of less than one indicate under-forecasts.

$$BIAS=(a+b)/(a+c) \quad (A5)$$

Skill Scores determine the average accuracy of a forecast compared to a reference forecast. The reference forecast could be a random forecast, or one based on climatological recurrence. Three different skill scores were computed for this study, Heidke Skill Score (HSS), Kuiper Skill Score (KSS), and the Equitable Threat Score (ETS) also known as the Gilbert Skill Score (Equations A6-A8).

The HSS is computed with a random reference forecast with the marginal distributions used to formulate the hit rate. It is the probability of a correct forecast by chance, both yes and no.

$$HSS = \frac{2 \cdot (ad - bc)}{(a + c)(c + d) + (a + b)(b + d)} \quad (A6)$$

Kuiper Skill Score is what is called an unBiased skill score, and is similar to the HSS; it especially rewards forecasts of rare events.

$$KSS = \frac{(ad - bc)}{(a + c)(b + d)} \quad (A7)$$

The final skill assessment done on the wind gust forecasts is the Equitable Threat Score (Dogget 1998). It is based upon the CSI and takes into account random chance forecast events. It is another increasing popular unBiased skill score.

$$ETS = \frac{(ad - bc)}{(ab + ac + ad + b^2 + bc + bd + c^2 + cd)} \quad (A8)$$

Finally, in order to ensure that the scores are statistically significant, a Chi-Square test was accomplished on all the two-by-two tables. A chi-square value of 6.637 is equivalent to a p-value of 0.01 (Devore 2000).

APPENDIX B

The data that follows is a two-by-two listing of each of the forecast times from the AFWA MM5 06 UTC run, for 23 surface stations in the T02B window. The grid resolution of the window is 15 km, and forecast times are every 3 hours. Two columns are listed, the first is the results for the WGE algorithm. The second is the current AFWA algorithm result.

The scores listed are Hit Rate, Critical Success Index (CSI), False Alarm Rate (FAR), Probability of Detection (POD), and Bias. Skill Scores are the Heidke Skill Score (HSS), the Kuipers Skill Score (KSS), and the Equitable Threat Score (ETS). The Chi-squared value is the value of the χ^2 statistic for the two by two tables.

Table B1 continued. The two-by-two matrices for the 06 UTC AFWA MM5 run. The scores are computed as in Appendix A.

12 Hour Forecast				15 Hour Forecast			
WGE		AFWA		WGE		AFWA	
89	53	142	119	65	64	129	92
69	360	429	39	58	350	408	31
158	413	571	158	123	414	537	123
		263	144			160	252
		308	269			254	285
		571	413			414	537
WGE AFWA				WGE AFWA			
Hit Rate:		0.786	0.680	Hit Rate:		0.773	0.644
CSI:		0.422	0.394	CSI:		0.348	0.325
POD:		0.563	0.753	POD:		0.528	0.748
FAR:		0.373	0.548	FAR:		0.496	0.635
BIAS ratio		0.899	1.665	BIAS ratio		1.049	2.049
HSS:		0.449	0.336	HSS:		0.368	0.264
KSS:		0.435	0.404	KSS:		0.374	0.361
Chi-Sqr.:		115.718	75.260	Chi-Sqr.:		72.621	49.755
ETS:		0.289	0.202	ETS:		0.225	0.152

Table B1 continued. The two-by-two matrices for the 06 UTC AFWA MM5 run. The scores are computed as in Appendix A.

<u>18 Hour Forecast</u>				<u>21 Hour Forecast</u>			
WGE		AFWA		WGE		AFWA	
46	141	187	208	48	210	258	133
30	346	376	279	11	267	278	344
76	487	563	487	59	477	536	477
			257				173
			306				363
			563				536
WGE AFWA				WGE AFWA			
Hit Rate:				Hit Rate:			
CSI:				CSI:			
POD:				POD:			
FAR:				FAR:			
BIAS ratio				BIAS ratio			
HSS:				HSS:			
KSS:				KSS:			
Chi-Sqr.:				Chi-Sqr.:			
ETS:				ETS:			

Table B1 continued. The two-by-two matrices for the 06 UTC AFWA MM5 run. The scores are computed as in Appendix A.

24 Hour Forecast				27 Hour Forecast			
WGE		AFWA		WGE		AFWA	
52	213	265	41	41	169	210	88
8	258	266	19	16	223	239	304
60	471	531	60	57	392	449	392
WGE				WGE			
AFWA				AFWA			
Hit Rate:				Hit Rate:			
CSI:				CSI:			
POD:				POD:			
FAR:				FAR:			
BIAS ratio				BIAS ratio			
HSS:				HSS:			
KSS:				KSS:			
Chi-Sqr.:				Chi-Sqr.:			
ETS:				ETS:			

Table B1 continued. The two-by-two matrices for the 06 UTC AFWA MM5 run. The scores are computed as in Appendix A.

30 Hour Forecast				33 Hour Forecast			
WGE		AFWA		WGE		AFWA	
35	196	231	224	59	58	117	135
20	289	309	316	31	194	225	207
55	485	540	540	90	252	342	342
WGE				WGE			
AFWA				AFWA			
Hit Rate:				Hit Rate:			
CSI:				CSI:			
POD:				POD:			
FAR:				FAR:			
BIAS ratio				BIAS ratio			
HSS:				HSS:			
KSS:				KSS:			
Chi-Sqr.:				Chi-Sqr.:			
ETS:				ETS:			

Table B1 continued. The two-by-two matrices for the 06 UTC AFWA MM5 run. The scores are computed as in Appendix A.

42 Hour Forecast						45 Hour Forecast					
WGE			AFWA			WGE			AFWA		
41	121	162	40	156	196	46	159	205	41	115	156
24	328	352	25	293	318	13	267	280	18	311	329
65	449	514	65	449	514	59	426	485	59	426	485
WGE						WGE					
Hit Rate:			AFWA			Hit Rate:			AFWA		
CSI:			0.648			0.645			0.726		
POD:			0.220			0.211			0.236		
FAR:			0.631			0.780			0.695		
BIAS ratio			0.747			0.776			0.737		
HSS:			2.492			3.475			2.644		
KSS:			0.221			0.197			0.249		
Chi-Sqr.:			0.361			0.406			0.425		
ETS:			34.337			35.079			42.893		
			0.124			0.109			0.142		

Table B1 continued. The two-by-two matrices for the 06 UTC AFWA MM5 run. The scores are computed as in Appendix A.

48 Hour Forecast					
WGE			AFWA		
89	53	142	119	144	263
69	360	429	39	269	308
158	413	571	158	413	571
		WGE	AFWA		
Hit Rate:		0.786	0.680		
CSI:		0.422	0.394		
POD:		0.563	0.753		
FAR:		0.373	0.548		
BIAS ratio		0.899	1.665		
HSS:		0.183	0.336		
KSS:		0.435	0.404		
Chi-Sqr.:		115.718	75.260		
ETS:		0.289	0.202		

APPENDIX C

The data that follows is a two-by-two listing of each of the forecast times from the AFWA MM5 18 UTC run, for 23 surface stations in the T02B CONUS window. The grid resolution of the window is 15 km, and forecast times are every 3 hours. Two columns are listed, the first is the results for the WGE algorithm. The second is the current AFWA algorithm result.

The scores listed are Hit Rate, Critical Success Index (CSI), False Alarm Rate (FAR), Probability of Detection (POD), and Bias. Skill Scores are the Heidke Skill Score (HSS), the Kuipers Skill Score (KSS), and the Equitable Threat Score (ETS). The Chi-squared value is the value of the χ^2 statistic for the two by two tables.

APPENDIX C. The 18 UTC AFWA MM5 WGE and AFWA Wind Gust Forecast Verification

Table C1. The two-by-two matrices for the 18 UTC AFWA MM5 run. The scores are computed as in Appendix A.

6 Hour Forecast						9 Hour Forecast					
WGE			AFWA			WGE			AFWA		
38	118	156	25	30	55	43	199	242	40	116	156
21	264	285	34	352	386	13	208	221	16	291	307
59	382	441	59	382	441	56	407	463	56	407	463
WGE						WGE					
Hit Rate:			AFWA			Hit Rate:			AFWA		
			0.685						0.542		
CSI:			0.215			CSI:			0.169		
POD:			0.644			POD:			0.768		
FAR:			0.756			FAR:			0.822		
BIAS ratio			2.644			BIAS ratio			4.321		
HSS:			0.198			HSS:			0.115		
KSS:			0.335			KSS:			0.279		
Chi-Sqr.:			25.114			Chi-Sqr.:			15.350		
ETS:			0.110			ETS:			0.061		

Table C1 continued. The two-by-two matrices for the 18 UTC AFWA MM5 run. The scores are computed as in Appendix A.

12 Hour Forecast				15 Hour Forecast			
WGE		AFWA		WGE		AFWA	
45	196	241	34	44	153	197	34
9	217	226	20	6	186	192	16
54	413	467	54	50	339	389	50
Hit Rate:		0.561		Hit Rate:		0.591	
CSI:		0.180		CSI:		0.217	
POD:		0.833		POD:		0.880	
FAR:		0.813		FAR:		0.777	
BIAS ratio		4.463		BIAS ratio		3.940	
HSS:		0.143		HSS:		0.190	
KSS:		0.359		KSS:		0.429	
Chi-Sqr.:		24.611		Chi-Sqr.:		32.033	
ETS:		0.077		ETS:		0.105	
WGE		AFWA		WGE		AFWA	
Hit Rate:		0.743		Hit Rate:		0.774	
CSI:		0.221		CSI:		0.279	
POD:		0.630		POD:		0.680	
FAR:		0.746		FAR:		0.679	
BIAS ratio		2.481		BIAS ratio		2.120	
HSS:		0.236		HSS:		0.317	
KSS:		0.387		KSS:		0.468	
Chi-Sqr.:		35.047		Chi-Sqr.:		48.061	
ETS:		0.134		ETS:		0.188	

Table C1 continued. The two-by-two matrices for the 18 UTC AFWA MM5 run. The scores are computed as in Appendix A.

18 Hour Forecast					21 Hour Forecast				
WGE		AFWA			WGE		AFWA		
34	72	106	24	68	60	68	128	63	77
16	267	283	18	275	28	251	279	25	242
50	339	389	42	343	88	319	407	88	319
WGE		AFWA			WGE		AFWA		
Hit Rate:		0.774	0.777		Hit Rate:		0.764	0.749	
CSI:		0.279	0.218		CSI:		0.385	0.382	
POD:		0.680	0.571		POD:		0.682	0.716	
FAR:		0.679	0.739		FAR:		0.531	0.550	
BIAS ratio		2.120	2.190		BIAS ratio		1.455	1.591	
HSS:		0.148	0.245		HSS:		0.402	0.391	
KSS:		0.468	0.373		KSS:		0.469	0.475	
Chi-Sqr.:		48.061	28.654		Chi-Sqr.:		70.268	68.826	
ETS:		0.188	0.140		ETS:		0.252	0.243	
WGE		AFWA			WGE		AFWA		
92	68	24	24	68	140	77	63	63	77
293	275	18	18	275	267	242	25	25	242
385	343	42	42	343	407	319	88	88	319

Table C1 continued. The two-by-two matrices for the 18 UTC AFWA MM5 run. The scores are computed as in Appendix A.

24 Hour Forecast				27 Hour Forecast			
WGE		AFWA		WGE		AFWA	
64	39	103	198	48	44	92	184
64	301	365	270	43	281	324	232
128	340	468	468	91	325	416	416
Hit Rate:				Hit Rate:			
CSI:				CSI:			
POD:				POD:			
FAR:				FAR:			
BIAS ratio				BIAS ratio			
HSS:				HSS:			
KSS:				KSS:			
Chi-Sqr.:				Chi-Sqr.:			
ETS:				ETS:			

Table C1 continued. The two-by-two matrices for the 18 UTC AFWA MM5 run. The scores are computed as in Appendix A.

<u>30 Hour Forecast</u>						<u>33 Hour Forecast</u>					
WGE			AFWA			WGE			AFWA		
39	103	142	43	142	185	38	154	192	33	95	128
23	269	292	18	231	249	10	212	222	15	271	286
62	372	434	61	373	434	48	366	414	48	366	414
WGE						WGE					
Hit Rate:			AFWA			Hit Rate:			AFWA		
CSI:						CSI:					
POD:						POD:					
FAR:						FAR:					
BIAS ratio						BIAS ratio					
HSS:						HSS:					
KSS:						KSS:					
Chi-Sqr.:						Chi-Sqr.:					
ETS:						ETS:					

Table C1 continued. The two-by-two matrices for the 18 UTC AFWA MM5 run. The scores are computed as in Appendix A.

<u>36 Hour Forecast</u>				<u>39 Hour Forecast</u>			
WGE		AFWA		WGE		AFWA	
40	170	210	82	36	130	166	54
9	214	223	302	8	204	212	280
49	384	433	384	44	334	378	334
			107				82
			326				296
			433				378
WGE AFWA				WGE AFWA			
Hit Rate:		0.587	0.755	Hit Rate:		0.635	0.815
CSI:		0.183	0.191	CSI:		0.207	0.286
POD:		0.816	0.510	POD:		0.818	0.636
FAR:		0.810	0.766	FAR:		0.783	0.659
BIAS ratio		4.286	2.184	BIAS ratio		3.773	1.864
HSS:		0.154	0.196	HSS:		0.195	0.345
KSS:		0.374	0.297	KSS:		0.429	0.475
Chi-Sqr.:		24.286	20.556	Chi-Sqr.:		29.046	51.570
ETS:		0.083	0.108	ETS:		0.108	0.209

Table C1 continued. The two-by-two matrices for the 18 UTC AFWA MM5 run. The scores are computed as in Appendix A.

<u>42 Hour Forecast</u>						<u>45 Hour Forecast</u>					
WGE			AFWA			WGE			AFWA		
29	141	170	22	70	92	53	72	125	66	68	134
12	240	252	19	311	330	41	286	327	28	290	318
41	381	422	41	381	422	94	358	452	94	358	452
WGE AFWA						WGE AFWA					
Hit Rate:			0.637	0.789		Hit Rate:			0.750	0.788	
CSI:			0.159	0.198		CSI:			0.319	0.407	
POD:			0.707	0.537		POD:			0.564	0.702	
FAR:			0.829	0.761		FAR:			0.576	0.507	
BIAS ratio			4.146	2.244		BIAS ratio			1.330	1.426	
HSS:			0.140	0.227		HSS:			0.323	0.443	
KSS:			0.337	0.353		KSS:			0.363	0.512	
Chi-Sqr.:			17.500	27.035		Chi-Sqr.:			48.957	93.642	
ETS:			0.075	0.128		ETS:			0.193	0.284	

Table C1 continued. The two-by-two matrices for the 18 UTC AFWA MM5 run. The scores are computed as in Appendix A.

48 Hour Forecast									
WGE			AFWA			AFWA			
65	43		108	81	86	167			
56	283		339	40	240	280			
121	326		447	121	326	447			
		WGE	AFWA						
Hit Rate:		0.779	0.718						
CSI:		0.396	0.391						
POD:		0.537	0.669						
FAR:		0.398	0.515						
BIAS ratio		0.893	1.380						
HSS:		0.419	0.362						
KSS:		0.405	0.406						
Chi-Sqr.:		79.107	62.040						
ETS:		0.265	0.221						

References

- AFWA Website 2002; MM5 Verification, <https://www.afwin.afwa.af.mil>.
- Arya, S. P. , 1988: *Introduction to Micrometeorology*. Academic Press, Inc. New York NY., 307 pp.
- Brasseur, O., 2001: Development and Application of a Physical Approach to Estimating Wind Gusts. *Mon. Wea. Review*, **129**, 5-25.
- Devore, J. L., 2000: *Probability and Statistics for Engineering and the Sciences, Fifth Edition*. Duxbury Press. CA., 775 .pp
- Dogget, K., 1988: “Glossary of Verification Terms”, www.sec.noaa.gov/forecast_verification/verif_glossary.html .
- Durst, C., 1960: Wind Speeds Over Short Periods of Time. *Meteor. Mag.*, **89**, 181-186.
- Ebisuzaki, W., 1999: WGRIB (Computer Program). National Center for Atmospheric Research.
- Garrat, J. R., 1992: *The Atmospheric Boundary Layer*. Cambridge Univ. Press, New York NY., 316 pp.
- Geerts, B., 2001: Estimating Downburst Related Maximum Wind Speeds by Means of Proximity Soundings in New South Wales, Australia. *Wea. Forecasting*, **16**, No. 2, 261-269.
- Glickman, T. S., (editor) 2001: *Glossary of Meteorology, Second Edition*. Amer. Meteor. Soc., Boston MA., 855 pp.
- Grell, G. A., J. Dudhia, and D. R. Stauffer, 1995: A Description of the Fifth-Generation Penn State / NCAR Mesoscale Model (MM5), NCAR Technical Note (NCAR / TN-398 +STR) June 1995, National Center for Atmospheric Research, Boulder CO.
- Hart, R. E., and G. S. Forbes, 1999: The Use of Model-Generated Soundings to Forecast Mesoscale Phenomena. Part II: An Initial Assessment in Forecasting Nonconvective Strong Wind Gusts. *Wea. Forecasting*, **14**, 461-469.
- Holton, J. R., 1992: *An Introduction to Dynamic Meteorology, Third Edition*. Academic Press, San Diego CA., 511 pp.
- Hong, Song-You and Pan, Hua-Lu, 1996: Non-Local Boundary Layer Vertical Diffusion in a Medium-Range Forecast Model. *Mon. Wea. Review*, **124**, No. 10, 2322-2339.

- McCann, D. W., 1994: WINDEX- A new index for forecasting microburst potential. *Wea. Forecasting*, **9**, 532-541.
- Miller, R. C., 1972: Notes on Analysis and Severe-Storm Forecasting Procedures of the Air Force Global Weather Central. *AWS TR 200 Revised*. Air Weather Service, USAF.
- Quinet, A., and J. Nemeghaire, 1991: Gust Forecasting (in French). Royal Meteorological Institute of Belgium Publ. 125, Vol. A, 57 pp.
- Sissenwine, N., 1973: Extreme Wind Speeds, Gustiness, and Variations with Height for MIL-STD-210B. *AFCRL-TR-73-0560*, Air Force Cambridge Research Laboratories, Hanscom Field MA.
- Sorbjan, Z., 1989: *Structure of the Atmospheric Boundary Layer*. Prentice-Hall, NJ., 317 pp.
- Stull, R. B. 1988: *An Introduction to Boundary Layer Meteorology*. Kluwer, Dordrecht, Germany., 666 pp.
- U.K. Met. Office, 1993: *Forecasters' Reference Book*. 191 pp.
- Unysis Website, 2002, "Archive of Surface Images", http://weather.unisys.com/archive/sfc_map/.
- Verkaik, J. W., 2000: Evaluation of Two Gustiness Models for Exposure Correction Calculations. *J. Appl. Meteor.*, **39**, 1613-1626.
- Waters, A. W., 1970: Forecasting Gusty Surface Winds in the Continental United States. *AWS TR 219*. Air Weather Service, USAF.
- Wilks, D. S., 1995: *Statistical Methods in the Atmospheric Sciences. An Introduction*. Academic Press, San Diego CA., 467 pp.

Vita

First Lieutenant Kevin W. LaCroix grew up in the “South.” He graduated from the Math, Science and Technology Center at the Paul Laurence Dunbar High School, Lexington, KY in 1994. He attended the University of South Alabama on a ROTC Meteorology Degree scholarship. He graduated with a Bachelor of Science degree in Geography with a concentration in Meteorology in 1998. Concurrently he was commissioned a Second Lieutenant in the United States Air Force.

Lt. LaCroix’s first assignment was the Joint Readiness Training Center (JRTC) and Fort Polk, LA. Here he served as the Staff Weather Officer for JRTC, and as a member of the Cadre Weather Team in support of the 2nd Armored Cavalry Regiment. While here, Lt. LaCroix participated in numerous exercises in a Joint environment, providing quality weather support to a broad spectrum of customers.

In August of 2000, Lt. LaCroix entered the graduate meteorology program in the School of Engineering at the Air Force Institute of Technology, Wright-Patterson, AFB. He is expected to graduate in March 2002.

REPORT DOCUMENTATION PAGE					<i>Form Approved OMB No. 0704-0188</i>				
The public reporting burden for this collection of information is estimated to average 1 hour per response, including the time for reviewing instructions, searching existing data sources, gathering and maintaining the data needed, and completing and reviewing the collection of information. Send comments regarding this burden estimate or any other aspect of this collection of information, including suggestions for reducing the burden, to Department of Defense, Washington Headquarters Services, Directorate for Information Operations and Reports (0704-0188), 1215 Jefferson Davis Highway, Suite 1204, Arlington, VA 22202-4302. Respondents should be aware that notwithstanding any other provision of law, no person shall be subject to any penalty for failing to comply with a collection of information if it does not display a currently valid OMB control number.									
PLEASE DO NOT RETURN YOUR FORM TO THE ABOVE ADDRESS.									
1. REPORT DATE (DD-MM-YYYY) 11-03-2002		2. REPORT TYPE Master's Thesis			3. DATES COVERED (From - To) June 2001-March 2002				
4. TITLE AND SUBTITLE APPLICATION OF THE WIND GUST ESTIMATE AND COMPARISON TO THE AFWA MM5 WIND GUST ALGORITHM					5a. CONTRACT NUMBER 5b. GRANT NUMBER 5c. PROGRAM ELEMENT NUMBER 5d. PROJECT NUMBER 5e. TASK NUMBER 5f. WORK UNIT NUMBER				
6. AUTHOR(S) LaCroix, Kevin, W., First Lieutenant, USAF					8. PERFORMING ORGANIZATION REPORT NUMBER AFIT/GM/ENP/02M-05				
7. PERFORMING ORGANIZATION NAME(S) AND ADDRESS(ES) Air Force Institute of Technology Graduate School of Engineering and Management (AFIT/EN)					10. SPONSOR/MONITOR'S ACRONYM(S) 11. SPONSOR/MONITOR'S REPORT NUMBER(S)				
9. SPONSORING/MONITORING AGENCY NAME(S) AND ADDRESS(ES) AFWA/DNXT ATTN: Mr. Bruce Telfeyan 106 Peacekeeper Dr. Offutt AFB, NE 68113-4039					12. DISTRIBUTION/AVAILABILITY STATEMENT APPROVED FOR PUBLIC RELEASE; DISTRIBUTION UNLIMITED				
13. SUPPLEMENTARY NOTES									
14. ABSTRACT The Air Force Weather Agency (AFWA) runs the Penn State/NCAR Mesoscale Model 5 (MM5) as their main mesoscale weather forecast model. One of the post-processing procedures is a diagnostic algorithm, which is used to help identify convective and non-convective wind gusts. O. Brassuer has identified a new Wind Gust Estimate (WGE), as a physically based method of computing non-convective wind gusts. The WGE surmises that Turbulent Kinetic Energy (TKE) transfers the momentum of faster upper-air winds to the surface, overcoming the buoyant energy of the surface layer. This work converts Brassuer's WGE to FORTRAN code and utilizing post-processed CONUS AFWA MM5 model output to estimate wind gusts by the WGE method. The WGE and AFWA methods are then categorically compared for accuracy and skill in forecasting wind gusts, to determine if the WGE method is superior to the current method. Three geographical regions are identified to determine gust sensitivities of the WGE and AFWA algorithms. The WGE generally performs better than the AFWA algorithm during daylight hours in correctly identifying and predicting gusts. Operational use of the WGE is warranted in the day and coastal regions, while improvements to the algorithm's handling of nighttime wind gusts is needed.									
15. SUBJECT TERMS wind gusts, meteorological models, boundary layer, turbulence, Turbulent Kinetic Energy, wind, weather									
16. SECURITY CLASSIFICATION OF: <table border="1" style="width: 100%; border-collapse: collapse; margin-top: 5px;"> <tr> <td style="width: 33%; padding: 2px;">a. REPORT U</td> <td style="width: 33%; padding: 2px;">b. ABSTRACT U</td> <td style="width: 33%; padding: 2px;">c. THIS PAGE U</td> </tr> </table>			a. REPORT U	b. ABSTRACT U	c. THIS PAGE U	17. LIMITATION OF ABSTRACT UU		18. NUMBER OF PAGES 980	
a. REPORT U	b. ABSTRACT U	c. THIS PAGE U							
			19a. NAME OF RESPONSIBLE PERSON Lt Col Michael K. Walters, Ph. D., USAF, ENP						
			19b. TELEPHONE NUMBER (Include area code) (937)255-3636, ext 4681						